Version of Record: https://www.sciencedirect.com/science/article/pii/S0223523424006494
Manuscript_9e6da4b1c1affc289dc9ba0e790ea49c

Indole-Core Inhibitors of Influenza A Neuraminidase: Iterative Medicinal Chemistry and Molecular Modeling

Andrey Tsedilin[1], Michaela Schmidtke[2], Natalia Monakhova[1], Irina Leneva[3], Irina Falynskova[3], Maria Khrenova[1,4], Thomas R. Lane[5], Sean Ekins[5], Vadim Makarov[1]*

[1] Federal Research Centre "Fundamentals of Biotechnology" of the Russian Academy of Sciences (Research Centre of Biotechnology RAS), Leninsky prospect, 33, build. 2, 119071 Moscow, Russia

[2] Institute of Medical Microbiology, Section of Experimental Virology, Jena University Hospital, Hans-Knöll-Straße 2, 07745 Jena, Germany

[3] Mechnikov Research Institute of Vaccines and Sera, Department of Virology, 105064 Moscow, Russia

[4] Chemistry Department, Lomonosov Moscow State University, 119991, Moscow, Russia

[5] Collaborations Pharmaceuticals, Inc., 840 Main Campus Drive, Lab 3510, Raleigh, NC27606, USA

*Corresponding author: makarov@inbi.ras.ru, +7 (495) 660-34-30 (195)

Abstract

Influenza viruses that cause seasonal and pandemic flu are a permanent health threat. The surface glycoprotein, neuraminidase, is crucial for the infectivity of the virus and therefore an attractive target for flu drug discovery campaigns. We have designed and synthesized more than 40 3-indolinone derivatives. We mainly investigated the role of substituents at the 2 position of the core as well as the introduction of substituents or a nitrogen atom in the fused phenyl ring of the core for inhibition of influenza virus neuraminidase activity and replication *in vitro* and *in vivo*. After evaluating the compounds for their ability to inhibit the viral neuraminidase, six potent inhibitors 3c, 3e, 7c, 12o, 12v, 18d were progressed to evaluate for cytotoxicity and inhibition of influenza virus A/PR/8/34 replication in in MDCK cells. Two hit compounds **3e** and **12o** were tested in an animal model of influenza virus infection. Molecular mechanism of the 3-indolinone derivatives interactions with the neuraminidase was revealed in molecular dynamic simulations. Proposed inhibitors bind to the 430-cavity that is different from the conventional binding site of commercial compounds. The most promising 3-indolinone inhibitors demonstrate stronger interactions with the neuraminidase in molecular models that supports proposed binding site.

Keywords

Influenza A, neuraminidase, 430-cavity, 7-Azaindole, Heumann cyclisation , 3-indolinone, anti-influenza drug discovery

Introduction

Seasonal flu is an acute respiratory infection caused by influenza viruses A and B, which affects nearly 10% of the global population every year [1]. Influenza viruses also constantly pose a pandemic threat due to their high mutation rate, virulence, fast transmissibility in humans, and zoonotic potential [2]. Therefore, discovery and development of novel antiviral drugs addressing influenza viruses are an urgent need. Among the main validated anti-influenza targets, neuraminidase has been extensively used for small-molecule drug discovery campaigns.

Neuraminidase is one of the major surface glycoproteins responsible for the infectivity of the virus. This enzyme releases viral particles from infected cells by cleaving sialic acid groups from glycoproteins [3-5]. To date, neuraminidase inhibitors including oseltamivir, zanamivir and peramivir are the drugs of choice for treating respiratory infection caused by influenza viruses [6]. Although these are effective against currently circulating strains of influenza A and B viruses, new strains resistant to these drugs may emerge suddenly due to specific mutations in the active site of neuraminidase and then spread rapidly around the world [7-9]. As a result, the search for new approaches towards influenza inhibition is continuously needed to combat such emerging strains of influenza viruses.

Influenza A virus neuraminidases form two genetically distinct groups: group-1 contains N1, N4, N5 and N8 subtypes while group-2 contains N2, N3, N6, N7 and N9 subtypes [10,11]. Among them, influenza viruses carrying N1 or N2 have circulated in humans, causing pandemics: Spanish flu (1918-1920), Russian flu (1977) and swine flu (2009) resulted from the H1N1 strain, Asian flu (1957-1958) came from the H2N2 strain, while Hong Kong flu (1968) is from the H3N2 strain. Another influenza A virus subtype, H5N1, which causes avian influenza, potentially poses a pandemic threat for the future and there are concerns about this currently [10,12].

The active site of influenza A virus N1 neuraminidase consists of a central sialic acid (SA) catalytic cavity surrounded by the two cavities termed the '150-cavity' and the '430-cavity' [13-15]. Being a key part of the neuraminidase active site, the SA catalytic cavity accommodates the SA moiety of the oligosaccharide substrate due to strong interactions with the arginine triad followed by the glycosidic bond cleavage [16,17]. The first neuraminidase inhibitors zanamivir and oseltamivir were developed to target this binding pocket [18,19]. The 150- and 430-cavities seem to play an important role in the dynamic process of ligand binding and represent promising 'hot spots' for rational drug design [14,15]. The 150-cavity is formed within 150-loop (residues 147-152) region in N1 neuraminidases and appears to close in response to zanamivir and oseltamivir binding [10, 13]. Yet, the lack of the 150-cavity in crystal structures of N2 and 2009 N1 neuraminidases [20] implies that inhibitors that are capable of binding at this site will be efficient only against specific neuraminidase variants. Another binding pocket, the 430-cavity, was identified within the 430-loop (residues 430-439) region using the computational solvent mapping approach [14, 21]. Molecular modeling studies of H5N1 neuraminidase indicate that the 430-cavity residues

may interact with SA and oseltamivir and affect their binding [22-24]. In contrast to the 150-cavity, the 430-cavity is featured in both N1 and N2 subtypes (Fig. 1) and is therefore a more attractive target for anti-influenza drug discovery.

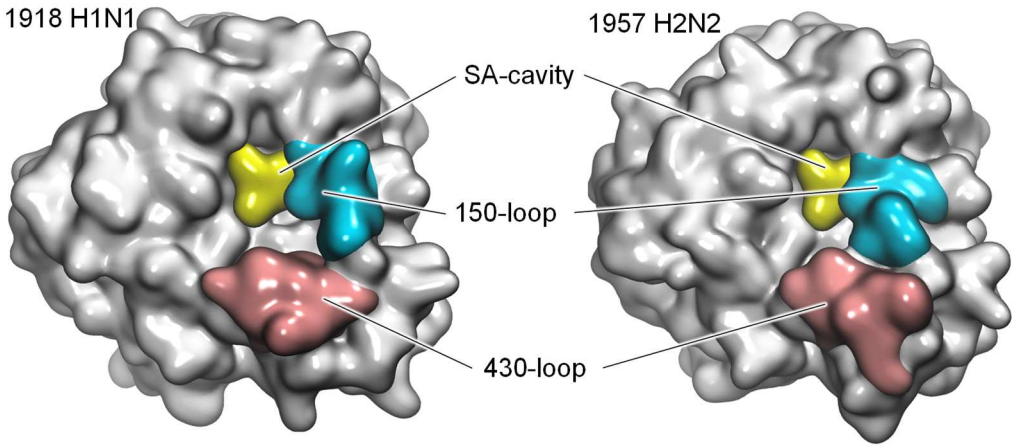

Figure 1. Localization of the 430-cavity in the N1 and N2 neuraminidase subtypes. Structures of H1N1 (PDB ID: 3BEQ) [13] and H2N2 (PDB ID: 3TIC) [25] neuraminidases are shown in grey surface representation. The SA cavity and the 150- and 430-loops are shown in yellow, cyan and pink surfaces, respectively. This figure was prepared with the Visual Molecular Dynamics (VMD) 1.9.4 software [26].

Several attempts have been made in recent years to develop small molecules that are able to occupy the 430-cavity (or both the SA- and 430-cavity) of influenza virus neuraminidase [27-32]. Research has been mainly focused on the modification of oseltamivir and zanamivir, and very few studies have utilized novel scaffolds to discover molecules that target the 430-cavity. As a result of high-throughput screening of our proprietary compound library, we identified 3-indolinone derivatives that inhibit influenza virus and subsequently determined that their target was neuraminidase. Further studies using machine learning techniques allowed us to optimise their structure and suggest that they interact with influenza virus neuraminidase in a 430-cavity. The 3-indolinones 3c, 3e, 7c, 12o, 12u, 12v and 18d were selected as the most interesting hits in the series with neuraminidase N1 interaction and two of them also showed in vivo efficacy in the influenza model.

Results and Discussion

Synthesis and anti-neuraminidase Activity of Target Compounds

Screening our in-house scaffold-diverse library for small molecules with anti-neuraminidase activity resulted in the selection of 3-indolinone-core compounds **1a-d** that inhibit influenza virus A/PR/8/34 (subtype H1N1) neuraminidase at micromolar concentrations in chemiluminescence (CL)-based enzyme inhibition assays (Table 1).

Table 1. Inhibition of influenza virus A/PR8/34 neuraminidase of the first series of methyleneindolin-3-ones **1-3**, **7** in a chemiluminescence--based assay

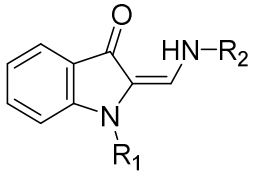

Cmpd	Substituents		IC_{50} values ± SD , µM[a]
	R_1	R_2	
1a	H	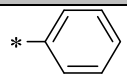	5.36 ± 2.33
1b	H	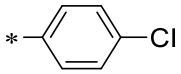	1.85 ± 0.64
1c	H	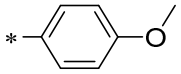	3.01 ± 0.81
1d	H	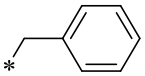	12.92 ± 6.81
2	Me	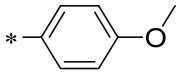	1.00 ± 0.18
3a	$COCH_3$	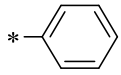	0.37 ± 0.30
3b	$COCH_3$	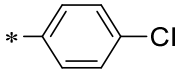	1.39 ± 0.80
3c	**$COCH_3$**	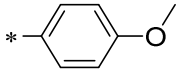	**0.10** ± 0.06
3d	$COCH_3$	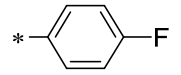	0.34 ± 0.00
3e	**$COCH_3$**	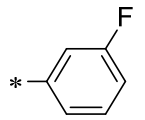	**0.03** ± 0.00
3f	$COCH_3$	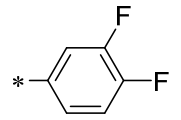	0.47 ± 0.43
7a	COC_2H_5	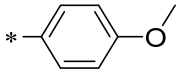	0.73 ± 0.32
7b	COC_2H_5	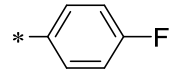	0.43 ± 0.12
7c	**COC_2H_5**	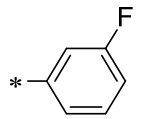	**0.23** ± 0.25

7d	COC_2H_5	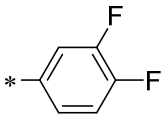	0.30 ± 0.26

[a]IC_{50}: 50% inhibition concentration. Values represent the mean and standard deviation of three independent experiments-

Based on these preliminary *in vitro* findings, a series of new 3-indolinones containing hydrophobic groups, such as propionyl- or acetyl- at the 1 position were synthesized and evaluated. In the second series of compounds, we focused on the introduction of various hydrophobic substituents on the 2-((phenylamino)methylene) moiety, expecting that this modification might be useful in enhancing anti-neuraminidase activity. Hence, we introduced one, two, or even three fluorine atoms or methoxy groups as well as an additional phenyl ring. The third series consists of molecules with a hydrophobic chlorine atom or a methoxy group at the 5 position. We also investigated the effect of scaffold hopping on neuraminidase inhibition. Therefore, a total of 40 novel new 3-indolinone-core compounds **7**, **12-14** and its analogues such as **18** were designed and evaluated for their anti-neuraminidase activity (Table 2).

Some desired compounds, 2-arylaminomethyleneindolin-3-ones **1a-c**, 1-acetyl-2-arylaminomethyleneindolin-3-ones **3a-c** were synthesized as described by Ryabova *et al*. [34]; 2-((benzylamino)methylene)indolin-3-one **1d** was obtained as described by Isakovich *et al*. [35]; and 2-(((4-methoxyphenyl)amino)methylene)-1-methylindolin-3-one **2** was synthesized as described by Sitkina *et al*. [36]. All physicochemical properties of our compounds synthesized correspond to those described earlier (see Experimental Section and Supplementary Materials).

The target 3-indolinone-based molecules **1-3**, **7, 12-14**, and **18** were prepared mainly according to three synthetic schemes (Schemes 1-3). 1-Substituted 2-((arylamino)methylene)indolin-3-ones **1a-d**, **2**, **3a-f**, **7a-d** were obtained via 4–5 steps according to Scheme 1. Commercially available anthranilic acid reacted with chloroacetic acid in the presence of sodium carbonate in aqueous medium to form *N*-(2-carboxyphenyl)glycine **4**. This intermediate was then *N*-acylated with acetic or propionic anhydrides or *N*-methylated with methyl iodide to give the corresponding *N*-substituted acids **5a-c**. The treatment of 2-(*N*-(substituted-methyl)propionamido)benzoic acids **5a-c** with acetic anhydride in the presence of triethylamine provide the intramolecular cyclization into 1-substituted-1*H*-indole-3-carboxylic acids ethyl ester **6a-c**. The final compounds **1a-d, 2, 3a-f and 7a-d** were prepared through *in situ* formation of enaminoketone using piperidine-carboxaldehyde dimetylacetal followed by transamination of the resulting intermediates with the corresponding anilines.

Scheme 1. Synthesis of 1-substituted 2-((arylamino)methylene)indolin-3-ones 1a-d, 2, 3a-f, and 7a-d.

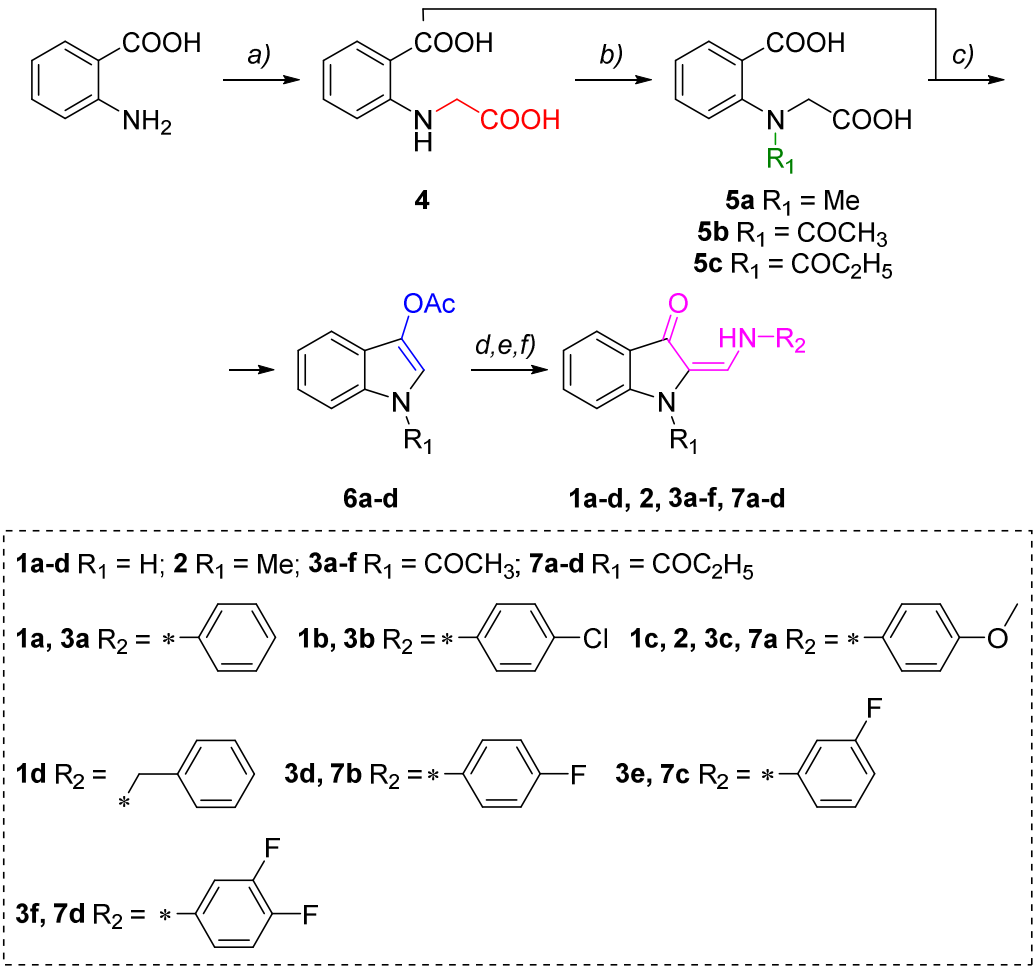

Reagents and condition: a) $ClCH_2COOH$, Na_2CO_3, H_2O; b) MeI or Ac_2O, or $(PrO)_2O$, Na_2CO_3, H_2O; c) $(AcO)_2O$, Et_3N; d) $POCl_3$, DMF, then KOH e) piperidine, piperidine-carboxaldehyde dimetylacetal, benzene, rt; f) the corresponding aniline, AcOH, iPrOH.

A slightly different synthetic scheme was used to afford the final 1-acetyl-3-indolinones **12-14** (Scheme 2). The 5-substituted 2-aminochloroacetophenones **8a-c** were prepared by the acylation of the corresponding commercial anilines using chloroacetonitrile in the presence of boron trichloride and aluminum trichloride as Lewis acid additives. Following acetylation of **8a-c** with acetic anhydride provides *N*-acetamides **9a-c**. These intermediates underwent intramolecular cyclization under basic condition in dimethoxyethane at room temperature, resulting in the corresponding *N*-substituted indolin-3-one **10a-c** with good yields. The reaction of **10a-c** with piperidine-carboxaldehyde dimetylacetal in benzene yielded and isolated the key intermediate enaminoketones **11a-c**. Compounds **11a-c** were then reacted with different anilines to provide the final products **12-14**.

Scheme 2. Synthesis of unsubstituted or 5-substituted 1-acetyl-2-((arylamino)methylene)indolin-3-ones 12a-x, 13a,b and 14a,b.

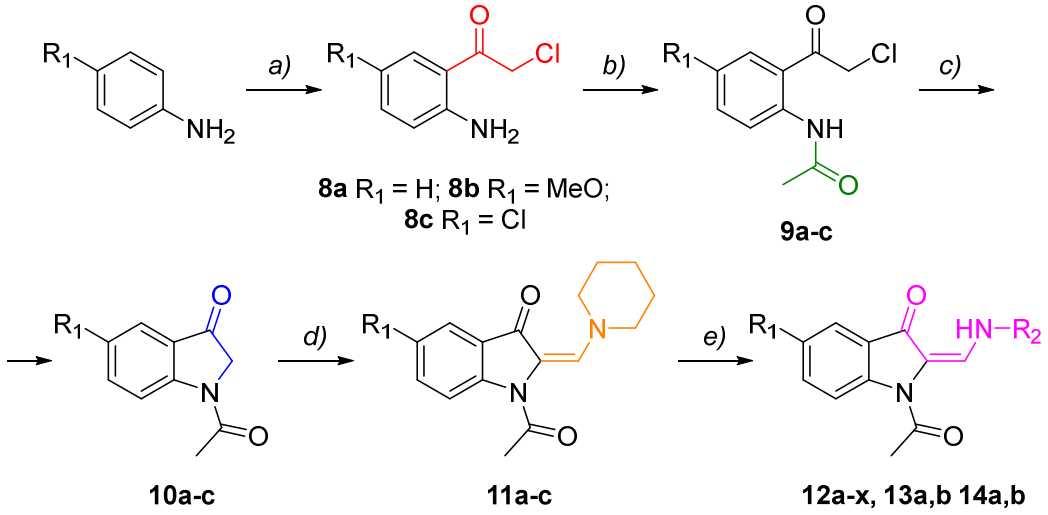

12a-x R_1 = H; **13a,b** R_1 = MeO; **14a,b** R_1 = Cl

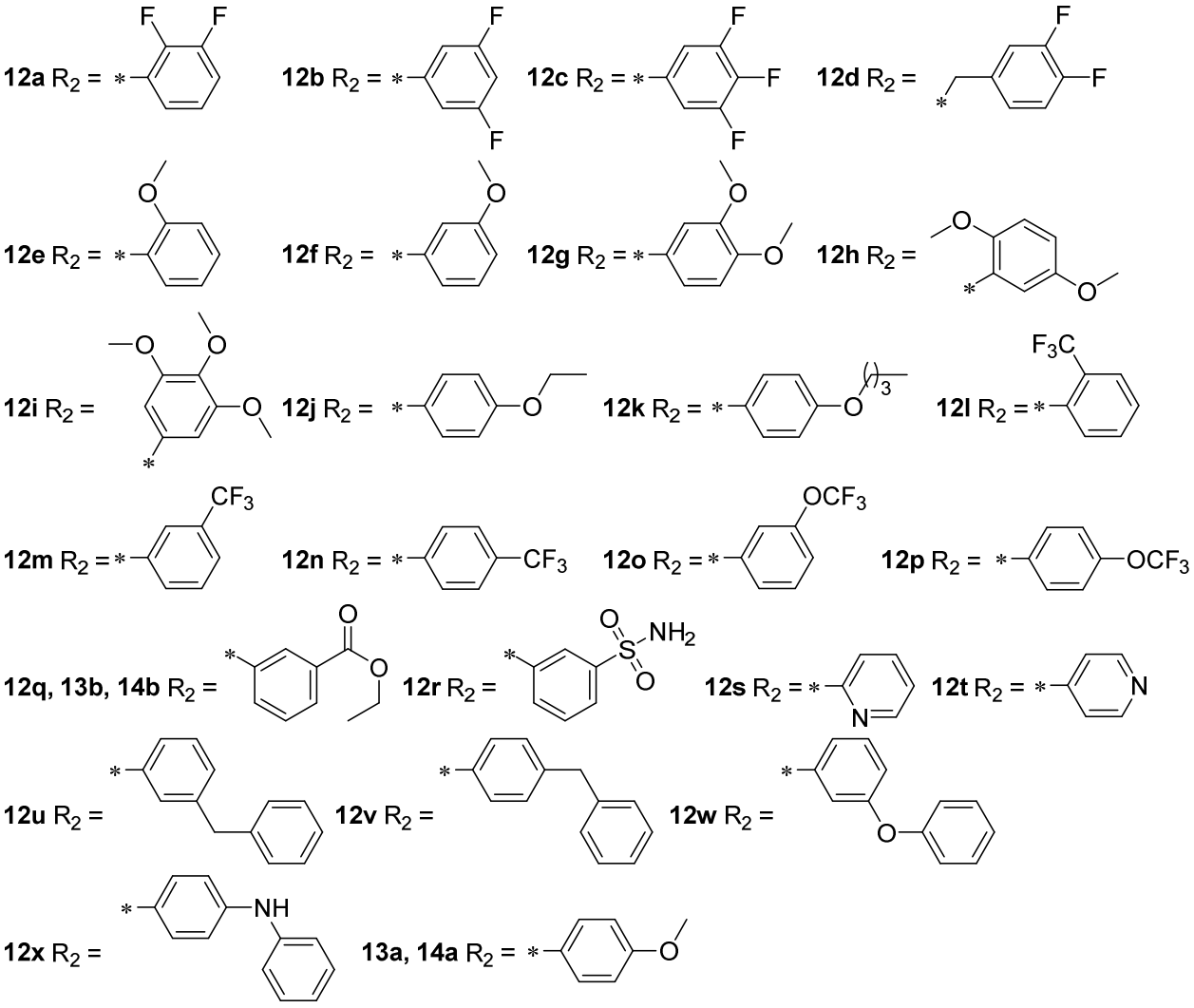

Reagents and condition: a) $ClCH_2CN$, BCl_3, $AlCl_3$, 0 °C then rt; b) Ac_2O, 80-85 °C; c) NaH, DME, 0 °C then rt; d) piperidine-carboxaldehyde dimetylacetal, piperidine, benzene, rt, e) the corresponding aniline, AcOH, iPrOH.

To investigate the role of the introduction of the nitrogen atom into the benzene ring of 3-indolinone, we synthesized four examples according to Scheme 3. For this, 7-azaindole-3-carboxaldehyde **15** was prepared from 7-azaindole under Duff reaction conditions. *N*-Acetylation of **15** provided intermediate **16**. *"m*-Chloroperoxybenzoic acid (*m*CPBA)-mediated Baeyer-Villiger oxidation of the formyl group of **16** led to formation of the corresponding formate intermediate, which upon hydrolysis converted to 1-(3-hydroxy-1H-pyrrolo[2,3-b]pyridin-1-yl)ethan-1-one, which in turn would tautomerize to 1-acetyl-1,2-dihydro-3H-pyrrolo[2,3-b]pyridin-3-one **17**. The desired products **18a-d** were obtained in the same way as described in Scheme 1.

Scheme 3. Synthesis of 1-acetyl-2-(((3-arylamino)methylene)-1,2-dihydro-3*H*-pyrrolo[2,3-*b*]pyridin-3-ones 18a-d.

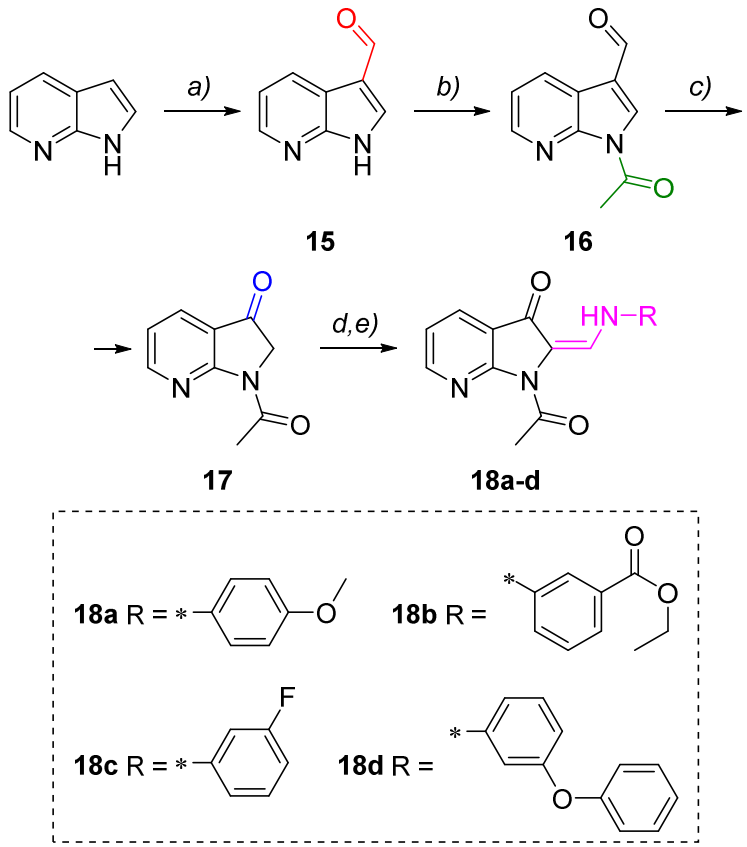

Reagents and condition: a) Hexamethylenetetramine, 33% AcOH, reflux; b) Ac_2O, Et_3N, DMAP, rt; c) *m*CPBA, CH_2Cl_2, 0 °C then rt; d) piperidine-carboxaldehyde dimetylacetal, benzene, rt; e) the corresponding aniline, AcOH, iPrOH.

Inhibition of Influenza A Virus Neuraminidase 1: Structure-Activity Relationships Analysis

All novel 3-indolinone derivatives were tested for their neuraminidase inhibitory activity using a chemiluminescence-based assay (Tables 1-3). In good agreement with previously published data oseltamivir was used as positive control, with mean IC_{50} values between 0.1-0.7 nM. As compounds **1a-d** exhibited weak inhibition of IVA neuraminidase, we introduced several

substituents at the 1 position of the 3-indolinone core in an effort to enhance the activity. As shown in Table 1, the introduction of the methyl group (**2**) slightly increases anti-neuraminidase activity. At the same time, compounds with 1-acetyl (**3a-f**) or 1-propionyl groups (**7b-d**) show significantly greater activity against neuraminidase with an IC_{50} range of 0.03-1.39 μM, suggesting that the bulky substituent is needed at this position.

In view of the equipotent activity of 1-acetyl- (**3a**) and 1-propionyl 3-indolinones (**7c**) against influenza neuraminidase, we chose the acetyl group for further structure-activity relationship exploration. In the second series of 3-indolinone-core compounds **12a-x**, we focused on studying the effect of various hydrophobic substituents on the 2-((phenylamino)methylene) moiety on enzyme inhibition (Table 3). No significant anti-neuraminidase activity was observed, when two or three fluorine atoms were introduced in various positions on the benzene ring (compounds **12a-d**). Compound **12f** with a methoxy group at the *meta* position demonstrates stronger neuraminidase inhibition than compound **12e** with an *ortho*-methoxy group. Surprisingly, while compound **12g** with a 3,4-dimethoxyphenyl fragment completely loses its anti-neuraminidase activity, compound **12h**, in which two methoxy groups switch to other positions on the benzene ring (2,5-position), exhibits modest anti-neuraminidase activity. Increasing the length of the alkyl side chain (compounds **12j**, **12k**) does not provide useful activity against the viral neuraminidase. The position of the trifluoromethyl group affects anti-neuraminidase activity, since the *meta*- and *para*-positions (**12m** and **12n**, respectively) of the group lead to a loss of activity compared to its *o*-position (compound **12l**). A different picture was observed in 3-indolinone-based compounds with a trifluoromethoxy group: compound **12o** with the *para*-position of the group which is more potent that compound **12p** with the *meta*-position.

Ethoxycarbonyl-containing compound **12q** exhibited good activity against the viral enzyme. Widely used in medicinal chemistry, the sulfonamide group usually serves as an H-bond acceptor and a hydrolysis-stable substituent [37]. In our case, the replacement of the ester group by this group leads to a decrease in anti-neuraminidase activity (compound **12r**).

The incorporation of a nitrogen atom into the benzene ring (compound **12s,t**) as an additional H-bond donor also led to a significant decrease in the neuraminidase inhibition, regardless of its position in the structure. The introduction of an additional hydrophobic benzene group positively influences the anti-neuraminidase activity of 3-indolinone derivatives (compounds **12u-x**); among them, compounds **12u** and **12v** containing a 3- or 4-benzylphenyl fragment show potent inhibition of H1N1 neuraminidase in the series of 3-indolinones.

Table 2. Inhibition of influenza virus A/PR/8/34 neuraminidase of the second series of 2-substitued 1-acetyl-methyleneindolin-3-ones **12.**

214

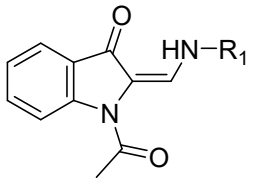

Cmpd	Substituent R	IC_{50} values ± SD , µM[a]
12a	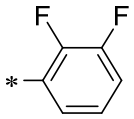	0.95 ± 0.32
12b	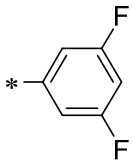	0.53 ± 0.18
12c	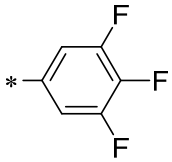	1.00 ± 0.46
12d	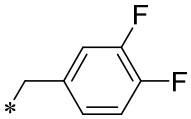	11.12 ± 1.51
12e	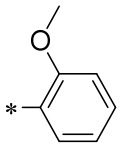	1.08 ± 0.82
12f	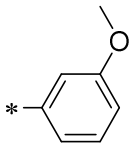	0.37 ± 0.23
12g	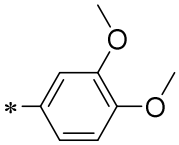	25.22 ± 17.49
12h	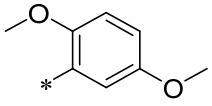	0.99 ± 0.59
12i	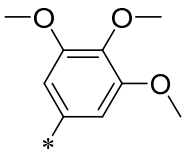	2.71 ± 0.49
12j	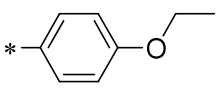	0.62 ± 0.25

12k	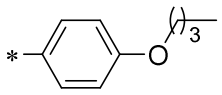	0.42 ± 0.39
12l	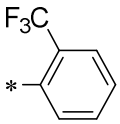	0.58 ± 0.29
12m	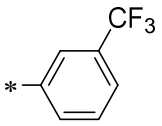	0.96 ± 0.67
12n	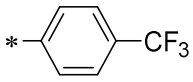	0.77 ± 0.17
12o	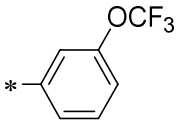	**0.20** ± 0.07
12p	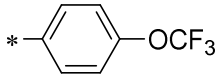	5.13 ± 2.16
12q	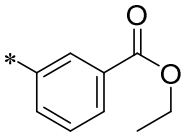	0.28 ± 0.28
12r	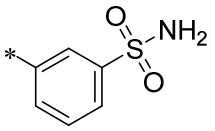	0.64 ± 0.49
12s	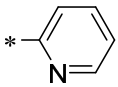	1.19 ± 0.41
12t	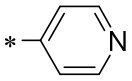	1.08 ± 0.36
12u	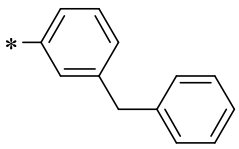	**0.20** ± 0.20
12v	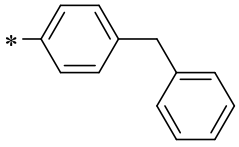	**0.10** ± 0.03
12w	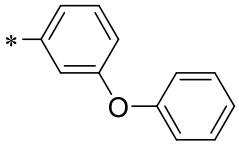	0.50 ± 0.32
12x	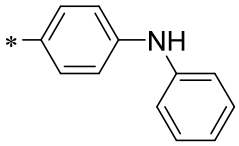	0.76 ± 0.28

[a] IC_{50}: 50% inhibition concentration. Values represent the mean and standard deviation of three independent experiments

Considering that the chlorine atom or methoxy groups in the indole ring provide substantial contributions to lipophilicity, we were interested in understanding their importance for influenza A virus neuraminidase inhibition. The introduction of these substituents at the 5 position of the core (compounds **13-14**) led to an approximately tenfold decrease in anti-NA activity compared to the activity of unsubstituted derivatives **3c** and **12q**, suggesting that only an unsubstituted benzene ring is required for a favorable level of inhibition.

It has recently been reported that 7-azaindole-containing pimodivir (VX-787) represents a potent *in vitro* and *in vivo* inhibitor of different influenza A virus strains, acting on the cap-snatching function of the PB2 subunit of the influenza A viral polymerase complex [38]. Although its clinical development was discontinued due to a lack of additional treatment benefits over the current standard-of-care drugs [39], its core could be useful in anti-influenza medicinal chemistry campaigns. Inspired by the idea of replacing the indole core with a bioisosteric 7-azaindole core, we synthesized and evaluated several compounds to test our hypothesis (Table 4). 7-azaindole-based compound **18** generally did not provide the required level of H1N1 neuraminidase inhibition while compound **18d**, containing a bulky lipophilic 3-benzylphenyl moiety at the 2 position, showed strong activity against neuraminidase 1. This finding also suggests an important role for the indole core in anti-neuraminidase activity.

Table 3. Inhibition of influenza virus A/PR/8/34 neuraminidase of the third series of methyleneindolin-3-ones **13** and **14**, and their bioisosteric analogues **18.**

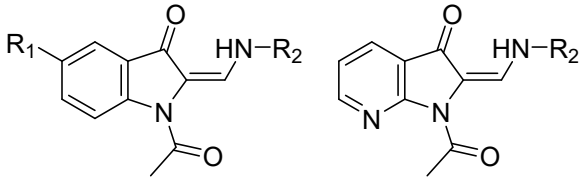

13,14 **18**

Cmpd	Substituents		IC_{50} values ± SD, µM
	R_1	R_2	
13a	MeO	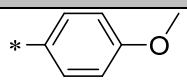	1.70 ± 0.62
13b	MeO	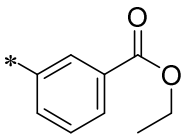	1.33 ± 0.81
14a	Cl	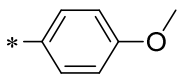	5.43 ± 3.36

14b	Cl	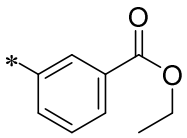	2.03 ± 1.26
18a	-	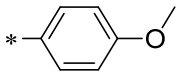	2.00 ± 1.00
18b	-	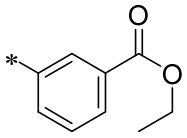	9.84 ± 6.93
18c	-	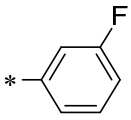	1.42 ± 0.82
18d	**-**	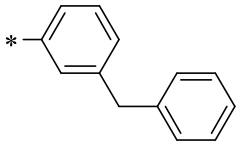	**0.15** ± 0.10

[a] IC_{50}: 50% inhibition concentration. Values represent the mean and standard deviation (SD) of three independent experiments

Because CL-based neuraminidase inhibition assays may reveal false-positive results, we wanted to confirm inhibition of viral neuraminidase activity for a panel of 3-indolinone derivatives with different IC_{50} values in complimentary cell-based assays [40]. The results summarised in Table S1 clearly demonstrate the lack of HA inhibition compared to NA inactivation, supporting neuraminidase N1 as a target for our compounds.

Prior to performing molecular dynamics (MD) simulations, we calculated several physicochemical properties for the selected compounds **3c**, **3e**, **7c**, **12o**, **12u**, **12v**, and **18d**, such as lipophilicity Log *P*, topological polar surface area (TPSA) values, and numbers of H-bond acceptors/donors using the SwissADME web tool. Interestingly, the two most potent molecules **3e** and **12v** have vastly different Log *P*, but similar TPSA. This suggests that hydrophobicity alone is not enough to drive potency.

Molecular basis of 3-indolinone derivative - neuraminidase complex formation

To get first insights into the binding mechanism and find a rational explanation behind the differences in IC_{50} values, we performed molecular dynamics (MD) simulations for hit compounds and several others with higher IC_{50} values.

The model system consisted of neuraminidase H1N1 and any of compounds **1a-d.** The source of coordinates of heavy atoms was a crystal structure PDB ID: 3B7E [13] that was a

complex of the enzyme with the zanamivir inhibitor that occupied the SA-cavity (Fig. 2). MD simulations predicted that compounds **1a-d** with the 3-indolinone-core interacted with the 430-loop and remained there until the end of the simulation in all the systems studied. Thus, the 3-indolinones **1a-d** are predicted to occupy an alternative neuraminidase binding site – the 430-cavity – in contrast to the commercial anti-influenza drugs, zanamivir and oseltamivir , that target the SA cavity (Fig. 2).

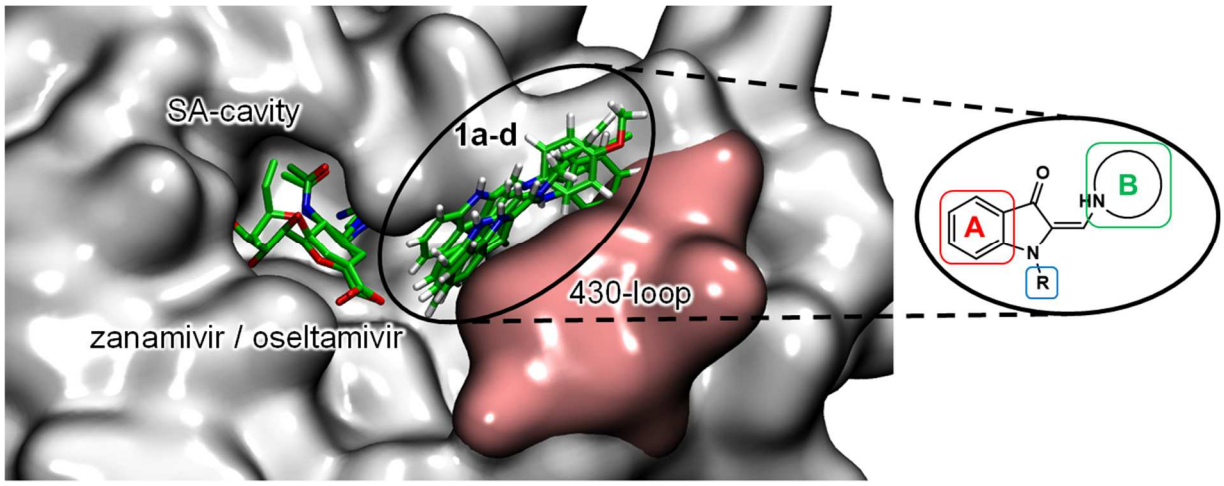

Figure 2. Predicted binding modes of 3-indolinones **1a-d** in neuraminidase N1 relative to zanamivir and oseltamivir. Neuraminidase N1 is shown as a grey surface, 430-loop is presented in pink. Zanamivir and oseltamivir are located in the crystal structures with the neuraminidase (PDB ID: 3B7E [13] and 6HP0 [33], respectively) and compounds **1a-d** configurations obtained in MD simulations are shown in stick representation. Atom color code: carbon – green, oxygen – red, nitrogen – blue and hydrogen – white. This figure was prepared using a VMD software [26].

We also compared the surface area of the three main N1 neuraminidase pockets (SA cavity, 150-cavity, and 430-cavity) to determine what molecular properties small-molecule inhibitors should have in order to bind to the 430-cavity and provide rational modifications of the 3-indolinone scaffold (Table 2). The comparison revealed that the SA cavity is the most polar site and slightly exceeds the volume of the other two cavities combined. The smallest 150-cavity is slightly more hydrophobic, characterized by high ratio of the polar solvent-accessible surface area (SASA) to the total cavity's SASA (59%). The 430-cavity is formed by hydrophobic residues Pro326, Trp403, Ile427, Pro431 and together with charged Arg371 and Lys432, it represents the most apolar site with the largest apolar SASA and the lowest polar SASA ratio (45%). The methylene groups of the Arg371 and Lys432 side chains are integrated into the hydrophobic pocket while the charged guanidinium and the amino groups are oriented towards the SA cavity and the bulk solvent. All these factors together likely favor the binding of hydrophobic small molecules like those from Table 1 in the 430-cavity.

Table 4. Comparison for the surface area of N1 neuraminidase pockets (PDB ID: 3BEQ).

Pocket	Total SASA, Å^2	Polar SASA, Å^2	Apolar SASA, Å^2	Volume, Å^3
SA cavity	444	310	134	870
150-cavity	223	131	92	336
430-cavity	286	129	157	510

Structure of H1N1 neuraminidase and **12u** complex obtained in MD simulations is shown on Figure 3. It shares the same binding patterns with complexes obtained with other compounds. In summary, from the experimental studies 1-acetyl (1-propionyl for the compound **3e**) and substituents of the phenyl core fragment B (Fig. 3) are likely important for the efficient complex formation.

The 1-acetyl or 1-propionyl moiety likely forms a stable hydrogen bond with the side chain of Ser370 that governs proper orientation of the 3-indolinone fragment relative to the side chain of the Trp403. It facilitates stabilization of the π-stacking interactions between the aromatic rings of the Trp403 residue and 3-indolinone. Also, binding of the core of these compounds is stabilized by hydrophobic interactions between their phenyl fragments and the side chain of the Ile427 residue.

Substituents in the phenyl core fragment B may bring different properties that eventually lowers the IC_{50} values further. One possibility is the introduction of the large hydrophobic moiety that is complementary to the binding site composed of the Pro431 residue, methylene fragments of the side chain of Gln430 and the side chain of Val149 residues. This is clearly observed for compounds **12u** (Fig. 3) and **12v**, **18d**. As the 430-cavity is exposed to solution, another possibility is to introduce a substituent to the phenyl core fragment B that may form hydrogen bonds with the solvent molecules and shield the compound core from the solution. Relevant examples from the set of hit compounds are the following: **12o**, **7c**, **3e**. For such interactions the *meta*- orientation of the substituent is more preferable than *para*- as the *meta*-substituent is mostly exposed to the solution. This pattern is observed if we compare hit compounds with their *para*-analogues **12p**, **7b** and **3d**.

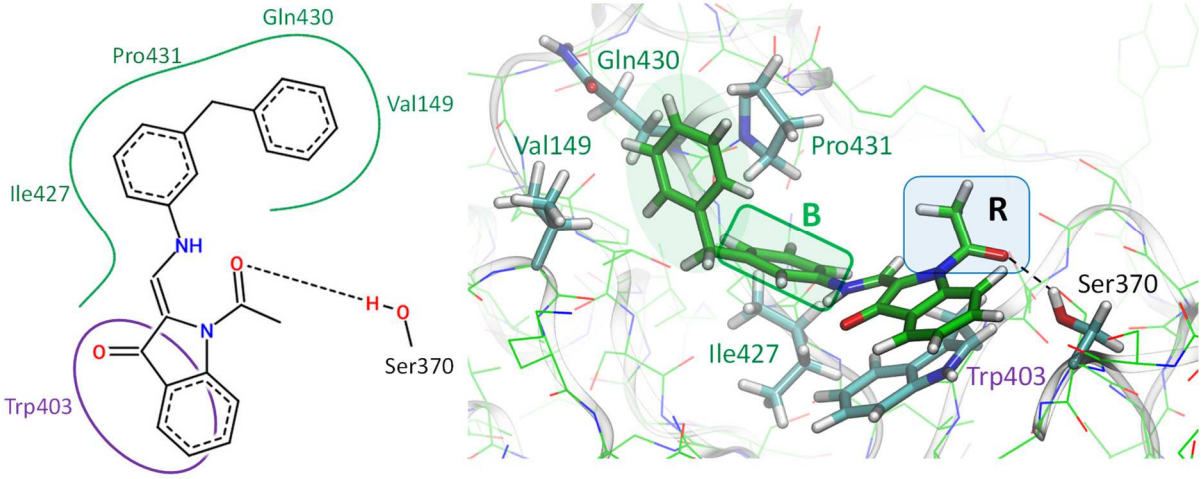

Figure 3. 2D and 3D representations of H1N1 neuraminidase and compound **12u** complex obtained in molecular dynamics Residues involved in hydrophobic interactions are marked green, π-stacking – violet, forming hydrogen bonds – black; hydrogen bond is shown with black dashed line. Compound moieties, a substituent of the phenyl core fragment B and R substituent, that are important for efficient binding, are highlighted green and blue, respectively. Color code: carbon – green for the compound and cyan for interacting residues, oxygen – red, nitrogen – blue and hydrogen – white.

Antiviral Activity of Selected Compounds against Influenza A Virus in Cell Culture

Given their acceptable inhibitory activity in the NA-enzyme assay, compounds **3c**, **3e**, **7c**, **12o**, **12v**, and **18d** were selected to test their *in vitro* activity in MDCK cells. We performed cytotoxicity assays with these compounds and evaluated their effect on influenza virus A/PR/8/34 replication in MDCK cells by comparing virus titers in the supernatant of untreated and treated cells (Table 6). Results from tetrazolium-based cytotoxicity assay showed that compounds **3c**, **3e**, **12v**, and **18d** were non-cytotoxic, whereas compounds **7c** and **12o** exhibited moderate cytotoxicity on the MDCK cell line. Compounds **12v** and **18d** were completely inactive *in vitro* against the influenza virus, and compounds **3c** and **7c** showed acceptable inhibitory activity (Table 6). The most potent compound against influenza neuraminidase, compound **3e**, inhibited the influenza infectious titer in cell culture at a moderate IC_{50} concentration. Another NA-active compound, **12o**, showed higher potency in inhibiting influenza virus A PR/8/34 (Table 6), suggesting that this molecule may inhibit influenza virus replication by binding to neuraminidase at the cellular level.

We have used public data from ChEMBL [55] for compounds screened against influenza H1N1 (CHEMBL613740) and neuraminidase (ChEMBL6135) to build Bayesian machine learning models with 5-fold receiver operating characteristic (ROC) values greater than 0.89 and other statistics were excellent (Figure S1). The phenotypic screening model was initially used to evaluate our most promising compounds with *in vitro* neuraminidase inhibition data and to aid select these compounds for *in vitro* phenotypic testing (Table 6). Compound **12r** had favorable predicted IC_{50} values that correlate with the observed inhibitory concentration against the virus in cell culture. We

have additionally compared different machine learning algorithms with the same public H1N1 and neuraminidase datasets using the same threshold (Figure S2A,B), as well as using these models to predict compounds in this study (Figure S2C). With a threshold of 10 μM, the predictions were accurate for several algorithms as well as for the consensus classification for neuraminidase inhibition.

While the results of these predictions did not appear to be useful for this class of compound, we then generated models limited to the molecules and data from this study alone (Figure S3). These models had reasonable cross validation statistics and therefore may be useful for future iterations and design.

Table 6. Cytotoxicity and anti-influenza A virus activity of selected compounds in MDCK cells

Cmpd	Cytotoxicity CC_{50}(MDCK), μM[a]	Inhibitory concentration IC_{50} (A/PR/8/34), μM[a]	Selectivity index SI[b]	Bayesian model[c]	Domain model[d]
3c	1814.42±230.26	12.00±3.20	151	0.47	0.60
3e	1479.63±302.57	33.80±6.80	44	0.47	0.58
7c	94.97±23.26	11.30±1.00	8	0.43	0.59
12o	104.92±30.58	3.00±0.80	35	0.48	0.51
12v	1740.24±239.35	111.40±16.30	16	0.44	0.56
18d	540.11±109.59	120.10±13.60	5	0.44	0.52

[a]The values represent the mean ± standard deviation (SD) of three independent experiments; [b]The selectivity index (SI) was defined as the ratio of CC_{50} to IC_{50}; [c]A score of 0.5 or greater is ideal for Bayesian model; [d]Higher domain values are preferred.

Comparison of the Efficacy of Compounds 3e and 12o in a Mouse Model of Influenza H1N1 Pneumonia

In preliminary efficacy studies, compounds **3e** and **12o** were administered orally at a dose of 50 mg/kg to assess their protection of BALB/c mice lethally challenged with A/California/04/2009 virus. The following endpoints were checked: virus titer in the lungs, body weigh changes, and survival rate. All negative-control mice (virus-infected and treated with saline) continuously lost body weight (Fig. 4C) and died from infection (100% mortality, Fig 4A) by day 11 after virus inoculation. Body weight loss was prevented in all animals treated either with compound **3e** or **12o** (Fig. 4A), and robust weight gain was observed during the study period. Treatment with either **3e** or **12o** resulted in a 30% survival rate, whereas oseltamivir provided a 50% survival rate in this mouse model (Fig. 4A). Treatment with either compound appeared to inhibit influenza virus replication in the lungs compared to the negative control, but these differences were non statistically significant. In addition, the virus was not completely eliminated from the lungs, and an increased dose or treatment duration may be required.

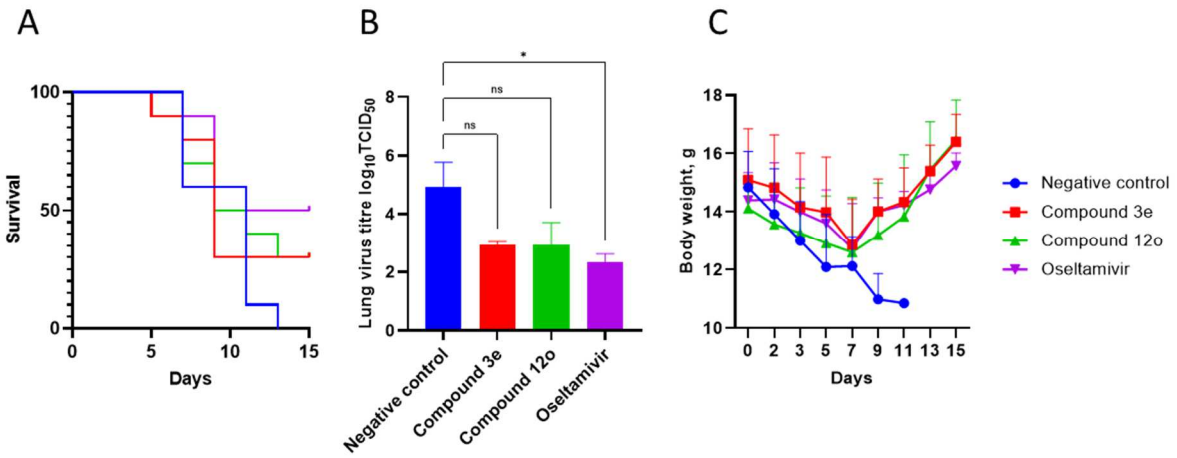

Figure 4. Efficacy studies in mice infected with influenza virus A/California/04/2009 (*n* = 10 per group). A) Survival plot; B) Results of lung virus titer determination on 4th day of infection (*n* = 3); c) Body weight change. *P ≤ 0.05.

Conclusion

Influenza viruses pose a health threat due to their high mutation rate and rapid transmissibility in humans. Of the established anti-influenza targets, neuraminidase appears to be the most valuable to date. Current commercial neuraminidase drugs, such as oseltamivir and zanamivir, are not without their known limitations. The development of new, improved inhibitors of the same enzyme therefore seems logical. Despite the highly polar SA cavity carrying the above-mentioned commercial drugs, neuraminidase has a smaller, mostly apolar binding site, the 430-cavity, which can also be a target for inhibitors. We propose 3-indolinone derivatives, describe their design, synthesis and inhibitory potency and suggest that this group of compound has bright perspective for future development. Molecular modelling shows that these compounds bind to the 430-cavity and specific inhibitor fragments responsible for the tight binding are determined. Hydrophobic, stacking and hydrogen bonding interactions determine binding efficiency and are most pronounced for the hits. Some more potent compounds, including 3c (0.24 μM), 3e (0.03 μM), 7c (0.23 μM), 12o (0.20 μM), 12u (0.20 μM), 12v (0.10 μM), 18d (0.15 μM), inhibited the neuraminidase enzyme in a CL-based assay and were then further evaluated in whole cell assays. Two promising compounds, 3e and 12o, were then evaluated in a mouse model of influenza A/California/04/2009 (H1N1)pdm09 virus infection, demonstrating efficacy and their potential for future development of this class of inhibitors as anti-influenza agents.

Experimental Section

Chemistry

General Methods

All reagents and solvents were purchased from commercial suppliers (AlfaAesar, Acros, Chimmed) and used without further purification. The ^{1}H and ^{13}C spectra were recorded on a Bruker

AC-200 NMR spectrometer (200 MHz, ^{1}H; 50 MHz, ^{13}C). Chemical shifts were measured in DMSO-d_6 or $CDCl_3$, using tetramethylsilane as an internal standard, and reported as ppm values. The following abbreviations are used to indicate multiplicity: s, singlet; d, doublet; t, triplet; q, quartet; quint, quintet; hex, hextet; m, multiplet; brs, broad singlet. Mass spectra were recorded on a Finnigan MAT INCOS 50 quadrupole mass spectrometer (EI, 70 eV) with direct injection. Purity of the final compounds were analyzed by analytical high-performance liquid chromatography (HPLC) on an Elute HPLC system (Bruker Daltonik GmbH, Heidelberg, Germany) equipped with an Azura UVD 2.1S UV detector (Knauer, Berlin, Germany) with a wavelength at 254 nm and acquisition rate at 1 Hz. Chromatographic separation was carried out on an Acquity HSS T3 column (2.1 × 100 mm, 1.3 µm, 100 Å) at 30 °C, sample injection volume – 2.0 µL. A mobile phase consisting 0.1 % formic acid in water (A), and 0.1 % formic acid in acetonitrile (B) was programmed with gradient elution of 30-95% at a flow rate of 250 µL/min. Data were processed with a Compass DataAnalysis 5.1 software (Bruker Daltonik). All final compounds were > 95 % pure. Elemental analysis (% C, H, N) was performed on an EURO EA elemental analyzer. Melting points were determined on an Electrothermal 9001 melting point apparatus (10 ºC per min) and were uncorrected. Merck KGaA silica gel 60 F_{254} plates were used for analytical thin-layer chromatography. Spots were detected by a UV lamp. Column chromatography was performed using a Merck 60 silica gel 60 (70-230 mesh). Yields refer to purified products and were not optimized.

N-(2-carboxyphenyl)glycine **4** was prepared from anthranilic acid and chloroacetic acid as described by Nuthakki *et al.* [41]. 2-(*N*-(Carboxymethyl)propionamido)benzoic acid **5** was synthesized from *N*-(2-carboxyphenyl)glycine **4** and propionic anhydride as described by Tighineanu *et al.* [42]. 2-Aminochloroacetophenones **8a-c**, *N*-(2-(2-chloroacetyl)phenyl)acetamides **9a-c** and the corresponding 1-acetyl-3-indolinones **10a-c** were obtained as described by Sugasawa *et al*. [43]. 1-Acetyl-2-(piperidin-1-ylmethylene)indolin-3-one **11a** was synthesized as described by Ryabova *et al.*, 5-methoxy- and 5-chloro-1-acetyl-2-(piperidin-1-ylmethylene)indolin-3-one **11b** and **c**, respectively, were synthesized in a similar manner from the corresponding 1-acetylindolin-3-ones [34]. 7-Azaindole-3-carboxaldehyde **15** was prepared in a similar way as described by Robinson [44]. Synthesis of 1-acetyl-1*H*-pyrrolo[2,3-*b*]pyridine-3-carbaldehyde **16** was carried out according to the procedure of Cheng *et al*. [45]. 1-Acetyl-1,2-dihydro-3*H*-pyrrolo[2,3-*b*]pyridin-3-one **17** was obtained as described by Desarbre and Mérour [46].

Synthetic Procedures

2-((Phenylamino)methylene)indolin-3-one **1a,** 2-(((4-chlorophenyl)amino)methylene)indolin-3-one **1b,** 2-(((4-methoxyphenyl)amino)methylene)indolin-3-one **1c** 1-acetyl-2-((phenylamino)methylene)-indolin-3-one **3a,** 1-acetyl-2-(((4-chlorophenyl)amino)methylene)indolin-3-one **3b** and 1-acetyl-2-(((4-methoxyphenyl)amino)methylene)indolin-3-one **3c** were synthesized according to [34], 2-((benzylamino)methylene)indolin-3-one **1d** was obtained according to [35] and 2-(((4-methoxyphenyl)-amino)methylene)-1-methylindolin-3-one **2** according to [36].

Synthesis of 1-R-1*H*-indol-3-yl acetate 6

To a mixture of acetic anhydride (10 eqv, 25 mL) and trimethylamine (2 eqv, 5 mL), benzoic acid **5** (1 eqv, 5 g) was added, and the reaction mixture was refluxed for 30 min. The reaction mixture was concentrated in vacuo, the residue was treated with water and extracted with dichloromethane (3-times). The combined organic phases were washed with water (3-times), dried over anhydrous Na_2SO_4, and concentrated in vacuo. The residue was purified by column chromatography using benzene as eluent (RF 0.6) to afford the product (2.25 g, 46 %) as a white solid.

General procedures for the synthesis of 1-propionyl-2-((arylamino)methylene)indolin-3-ones 7a-d

A mixture of 1-R-1*H*-indol-3-yl acetate **6** (1 eqv) was transformed into corresponding indoline-3-on as described in [36] but fithout additional purification via recrystallization, piperidine (1.5 eqv) and piperidine-carboxaldehyde dimetylacetal (3 eqv) in benzene (5 mL) were added and the reaction mixture was refluxed for 3 h, concentrated *in vacuo*, and to the residue (1 eqv) was added the corresponding aniline (1.2 eqv), AcOH (2.5 mL) in isopropanol (5 mL). The reaction mixture was refluxed for 20 min. After cooling to rt, the precipitate was filtered off, washed with isopropanol and ethyl ether, and recrystallized from isopropanol to afford the corresponding product **7a-d**.

1-Propionyl-2-(((4-methoxyphenyl)amino)methylene)indolin-3-one **7a**

Yield 0.15 g (50 %), white solid, mp. 184-185 °C. ^{1}H NMR (DMSO-d_6; δ, ppm): 1.20 (3H, t, *J* = 7.1 Hz, C$\underline{H_3}$CH$_2$CO), 3.05 (2H, q, *J* = 7.0 Hz, CH$_3$C$\underline{H_2}$CO), 3.76 (3H, s, CH$_3$O), 6.99 (2H, d, *J* = 8.9 Hz, 2CH$_{ar}$), 7.14-7.46 (3H, m, 3CH$_{ar}$), 7.55-7.73 (1H, m, CH$_{ar}$), 7.79 (1H, d, *J* = 7.6 Hz, 4-CH$_{ar}$), 7.96 (1H, d, *J* = 8.6 Hz, 7-CH$_{ar}$), 9.04 (1H, brs, CH), 11.96 (1H, brs, NH). ^{13}C NMR (DMSO-d_6; δ, ppm): 8.7, 30.8, 55.2, 115.0, 115.8, 116.5, 117.8, 122.1, 123.1, 125.0, 132.9, 137.0, 142.4, 156.0, 172.0. MS (EI; rel. int., %): m/z 294 (M$^+$, 91). Anal. calcd for $C_{18}H_{18}N_2O_2$: C, 73.45; H, 6.16; N, 9.52. Found: C, 73.57; H, 6.23; N, 9.61.

1-Propionyl-2-(((4-fluorophenyl)amino)methylene)indolin-3-one **7b**

Yield 0.03 g (36 %), white solid, mp.146-148 °C. ^{1}H NMR (DMSO-d_6; δ, ppm): 1.19 (3H, t, *J* = 7.1 Hz, C$\underline{H_3}$CH$_2$CO), 3.05 (2H, q, *J* = 7.1 Hz, CH$_3$C$\underline{H_2}$CO), 7.09-7.55 (5H, m, 5CH$_{ar}$), 7.68 (1H, t, *J* = 7.8 Hz, 5-CH$_{ar}$), 7.79 (1H, d, *J* = 7.5 Hz, 4-CH$_{ar}$), 7.97 (1H, d, *J* = 8.5 Hz, 7-CH$_{ar}$), 9.02 (1H, brs, CH), 11.90 (1H, brs, NH). ^{13}C NMR (DMSO-d_6; δ, ppm): 8.9, 31.0, 116.2, 116.4, 116.7, 116.9, 118.3, 118.5, 122.5, 123.5, 124.1, 124.9, 127.2, 127.7, 133.6, 136.4, 136.4, 136.7, 143.0, 156.3, 161.1, 172.3, 180.1. MS (EI; rel. int., %): m/z 310 (M$^+$, 88). Anal. calcd for $C_{18}H_{15}FN_2O_2$: C, 69.67; H, 4.87; N, 9.03. Found: C, 69.74; H, 4.93; N, 9.08.

1-Propionyl-2-(((3-fluorophenyl)amino)methylene)indolin-3-one **7c**

Yield 0.05 g, (16 %), white solid, mp. 118-120 °C. ^{1}H NMR (DMSO-d_6; δ, ppm): 1.18 (3H, t, *J* = 7.1 Hz, C$\underline{H_3}$CH$_2$CO), 2.97 (2H, q, *J* = 7.5 Hz, CH$_3$C$\underline{H_2}$CO), 6.90 (1H, t, *J* = 8.4 Hz, 1CH$_{ar}$), 7.00-

7.54 (4H, m, 4CH_{ar}), 7.54-7.84 (2H, m, 2CH_{ar}), 7.92 (1H, d, *J* = 8.4 Hz, 7-CH_{ar}), 8.95 (1H, brs, CH), 11.77 (1H, brs, NH). ^{13}C NMR (DMSO-d_6; δ, ppm): 8.9, 31.0, 103.2, 103.8, 109.8, 110.2, 112.5, 116.9, 122.6, 123.5, 124.6, 131.3, 131.5, 133.9, 135.3, 141.7, 141.9, 143.4, 160.6, 165.5, 172.3, 180.7. MS (EI; rel. int., %): m/z 310 (M^+, 85). Anal. calcd for $C_{18}H_{15}FN_2O_2$: C, 69.67; H, 4.87; N, 9.03. Found: C, 69.59; H, 4.82; N, 8.97.

1-Propionyl-2-(((3,4-difluorophenyl)amino)methylene)indolin-3-one **7d**

Yield 0.067 g (17 %), white solid, mp. 149-150 °C. ^{1}H NMR (DMSO-d_6; δ, ppm): 1.17 (3H, t, *J* = 7.1 Hz, C$\underline{H_3}$CH_2CO), 2.97 (2H, q, *J* = 7.5 Hz, CH_3C$\underline{H_2}$CO), 6.95-7.20 (1H, m, CH_{ar}), 7.20-7.57 (3H, m, 3CH_{ar}), 7.57-7.83 (2H, m, 2CH_{ar}), 7.92 (1H, d, *J* = 8.5 Hz, 7-CH_{ar}), 8.87 (1H, brs, CH), 11.71 (1H, brs, NH). ^{13}C NMR (DMSO-d_6; δ, ppm): 8.9, 25.4, 31.0, 106.8, 106.2, 112.8, 112.9, 116.8, 116.8, 118.1, 118.5, 122.5, 122.8, 123.5, 124.1, 124.6, 133.8, 135.7, 137.1, 137.3, 143.2, 143.3, 143.5, 147.4, 147.6, 148.0, 148.3, 152.2, 152.5, 172.2, 180.5. MS (EI; rel. int., %): m/z 328 (M^+, 90). Anal. calcd for $C_{18}H_{14}F_2N_2O_2$: C, 65.85; H, 4.30; N, 8.53. Found: C, 65.78; H, 4.23; N, 8.57.

General procedures for the synthesis of 1-acetyl-2-((arylamino)methylene)indolin-3-ones 3d-f, 12a-x, 13a-b and 14a-b

A mixture of 1-R-1*H*-indol-3-yl acetate **6d** or corresponding 1-acetyl-2-(piperidin-1-ylmethylene)indolin-3-one **11a-c** (1 eqv), the corresponding aniline (1.1 eqv) and AcOH (3.0 mL) in isopropanol (6 mL) was refluxed for 20-30 min or stirred at rt for 2-3 h. After cooling to rt, the precipitate was filtered off, washed with isopropanol and diethyl ether, and recrystallized from the corresponding solvent to afford the corresponding product **3d-f, 12a-x 13a-b or 14a-b**.

1-Acetyl-2-(((4-fluorophenyl)amino)methylene)indolin-3-one **3d**

Yield 0.2 g (68 %), white solid, mp. 167-168 °C (isopropanol). ^{1}H NMR (DMSO-d_6; δ, ppm): 2.69 (3H, s, CH_3CO), 7.29 (5H, m, CH, 4CH_{ar}), 7.56-7.88 (2H, m, 2CH_{ar}), 7.94 (1H, d, *J* = 8.5 Hz, 7-CH_{ar}), 8.93 (1H, d, *J* = 9.6 Hz, CH), 11.81 (1H, d, *J* = 11.4 Hz, NH). ^{13}C NMR (DMSO-d_6; δ, ppm): 26.8, 116.2, 116.6, 116.7, 118.2, 118.4, 122.4, 123.6, 124.8, 133.5, 136.5, 143.2, 156.3, 161.1, 168.6, 180.0. MS (EI; rel. int., %): m/z 296 (M^+, 69). Anal. calcd for $C_{17}H_{13}FN_2O_2$: C, 68.91; H, 4.42; N, 9.45. Found: C, 68.85; H, 4.34; N, 9.37.

1-Acetyl-2-(((3-fluorophenyl)amino)methylene)indolin-3-one **3e**

Yield 0.13 g (44 %), white solid, mp 122-123 °C (methanol). ^{1}H NMR (DMSO-d_6; δ, ppm): 2.67 (3H, s, CH_3CO), 6.89 (1H, t, *J* = 7.7 Hz, 5-CH_{ar}), 6.99-7.54 (4H, m, 4CH_{ar}), 7.54-7.84 (2H, m, 2CH_{ar}), 7.93 (1H, d, *J* = 8.5 Hz, 7-CH_{ar}), 8.91 (1H, brs, CH), 11.73 (1H, s, NH). ^{13}C NMR (DMSO-d_6; δ, ppm): 26.8, 103.2, 103.7, 109.8, 110.2, 112.4, 116.5, 116.8, 122.5, 123.6, 124.7, 131.3, 131.5, 133.8, 135.1, 141.6, 141.8, 143.5, 160.6, 165.4, 168.6, 180.6. MS (EI; rel. int., %): m/z 296 (M^+, 75). Anal. calcd for $C_{17}H_{13}FN_2O_2$: C, 68.91; H, 4.42; N, 9.45. Found: C, 68.88; H, 4.51; N, 9.50.

1-Acetyl-2-(((3,4-difluorophenyl)amino)methylene)indolin-3-one **3f**

Yield 0.18 g (62%), white solid, mp 168-169 °C (isopropanol). ^{1}H NMR (DMSO-d_6; δ, ppm): 2.66 (3H, s, CH_3CO), 7.08 (1H, d, *J* = 8.9 Hz, 2'-CH_{ar}), 7.20-7.54 (3H, m, 3CH_{ar}), 7.54-7.80 (2H, m, 2CH_{ar}), 7.91 (1H, d, *J* = 8.5 Hz, 7-CH_{ar}), 8.80 (1H, s, CH), 11.65 (1H, brs, NH). ^{13}C NMR (DMSO-

d_6; δ, ppm): 26.6, 105.9, 106.3, 112.9, 112.9, 113.0, 113.0, 116.5, 116.9, 118.1, 118.5, 122.5, 123.6, 124.7, 133.8, 135.6, 137.2, 143.7, 168.5, 180.6. MS (EI; rel. int., %): m/z 314 (M^+, 85). Anal. calcd for $C_{17}H_{12}F_2N_2O_2$: C, 64.97; H, 3.85; N, 8.91. Found: C, 65.05; H, 3.91; N, 8.83.

1-Acetyl-2-(((2,3-difluorophenyl)amino)methylene)indolin-3-one **12a**

Yield 0.07g (24 %), white solid, mp 176-177 °C (isopropanol). ^{1}H NMR (DMSO-d_6; δ, ppm): 2.68 (3H, s, CH_3CO), 6.90-4.49 (4H, m, $4CH_{ar}$), 7.50-8.05 (3H, m, $3CH_{ar}$), 8.93 (1H, brs, CH), 11.90 (1H, brs, NH). ^{13}C NMR (DMSO-d_6; δ, ppm): 26.3, 110.6, 110.9, 11.6, 16.2, 117.5, 122.5, 123.4, 124.2, 124.9, 125.0, 125.1, 125.2, 129.9, 130.0, 133.9, 134.1, 137.5, 137.8, 142.4, 142.7, 143.7, 147.5, 147.7, 152.3, 152.5, 168.1, 181.3. MS (EI; rel. int., %): m/z 314 (M^+, 77). Anal. calcd for $C_{17}H_{12}F_2N_2O_2$: C, 64.97; H, 3.85; N, 8.91. Found: C, 64.88; H, 3.75; N, 9.01.

1-Acetyl-2-(((3,5-difluorophenyl)amino)methylene)indolin-3-one **12b**

Yield 0.07 g (24 %), white solid, mp 209-210 °C (isopropanol). ^{1}H NMR (DMSO-d_6; δ, ppm): 2.67 (3H, s, CH_3CO), 6.82 (1H, tt, J = 9.3 Hz, 2.2, 4'-CH_{ar}), 6.93-7.18 (2H, m, $2CH_{ar}$), 7.30 (1H, t, J = 7.4 Hz, 5-CH_{ar}), 7.51-7.84 (2H, m, $2CH_{ar}$), 7.95 (1H, d, J = 8.5 Hz, 7-CH_{ar}), 8.77 (1H, brs, CH), 11.58 (1H, brs, NH). ^{13}C NMR (DMSO-d_6; δ, ppm): 26.2, 97.4, 97.9, 99.3, 99.7, 99.9, 116.3, 117.1, 122.3, 123.4, 124.2, 133.8, 133.9, 144.0, 168.3, 181.0. MS (EI; rel. int., %): m/z 314 (M^+, 81). Anal. calcd for $C_{17}H_{12}F_2N_2O_2$: C, 64.97; H, 3.85; N, 8.91. Found: C, 64.86; H, 3.72; N, 8.84.

1-Acetyl-2-(((3,4,5-trifluorophenyl)amino)methylene)indolin-3-one **12c**

Yield 0.05 g (16 %), white solid, mp 184-185 °C (isopropanol). ^{1}H NMR (DMSO-d_6; δ, ppm): 2.67 (3H, s, CH_3CO), 6.99-7.52 (3H, m, $3CH_{ar}$), 7.52-7.87 (2H, m, $2CH_{ar}$), 7.97 (1H, d, J = 8.5 Hz, 7-CH_{ar}), 8.71 (1H, brs, CH), 11.55 (1H, brs, NH). ^{13}C NMR (DMSO-d_6; δ, ppm): 26.7, 95.4, 101.2, 101.7, 116.7, 117.2, 122.6, 123.7, 124.4, 126.3, 127.9, 132.4, 134.2, 134.6, 136.7, 137.3, 144.0, 148.4, 153.3, 168.6, 181.0. MS (EI; rel. int., %): m/z 332 (M^+, 76). Anal. calcd for $C_{17}H_{11}F_3N_2O_2$: C, 61.45; H, 3.34; N, 8.43. Found: C, 61.53; H, 3.27; N, 8.36.

1-Acetyl-2-(((3,4-difluorobenzyl)amino)methylene)indolin-3-one **12d**

Yield 0.10 g (31 %), white solid, mp 154-155 °C (ethyl acetate). ^{1}H NMR (DMSO-d_6; δ, ppm): 2.62 (3H, s, CH_3CO), 4.62 (2H, brs, CH_2), 6.91-8.16 (7H, m, $7CH_{ar}$), 8.66 (1H, brs, CH), 10.35 (1H, brs, NH). ^{13}C NMR (DMSO-d_6; δ, ppm): 26.9, 50.7, 114.2, 116.4, 116.8, 117.5, 117.8, 122.0, 123.2, 124.2, 124.3, 125.6, 132.5, 136.6, 142.0, 146.4, 168.1, 178.3. MS (EI; rel. int., %): m/z 328 (M^+, 76). Anal. calcd for $C_{18}H_{14}F_2N_2O_2$: C, 65.85; H, 4.30; N, 8.53. Found: C, 65.92; H, 4.38; N, 8.49.

1-Acetyl-2-(((2-methoxyphenyl)amino)methylene)indolin-3-one **12e**

Yield 0.18 g (58 %), white solid, mp 179-180 °C (isopropanol). ^{1}H NMR (DMSO-d_6; δ, ppm): 2.68 (3H, s, CH_3CO), 3.93 (3H, s, CH_3O), 6.86-7.52 (5H, m, $5CH_{ar}$), 7.63 (1H, t, J = 7.7 Hz, 5-CH_{ar}), 7.77 (1H, d, J = 7.5 Hz, 7-CH_{ar}), 9.03 (1H, d, J = 12.6 Hz, CH), 12.02 (1H, d, J = 12.7 Hz, NH). ^{13}C NMR (DMSO-d_6; δ, ppm): 26.9, 56.0, 111.7, 113.3, 116.5, 116.9, 121.4, 122.5, 123.6, 123.9, 125.0, 128.7, 133.4, 134.7, 143.1, 148.0, 168.6, 180.0. MS (EI; rel. int., %): m/z 308 (M^+, 83). Anal. calcd for $C_{18}H_{16}N_2O_3$: C, 70.12; H, 5.23; N, 9.09. Found: C, 70.23; H, 5.14; N, 9.01.

1-Acetyl-2-(((3-methoxyphenyl)amino)methylene)indolin-3-one **12f**

Yield 0.14 g (46 %), white solid, mp 104-105 °C (isopropanol). ^{1}H NMR (DMSO-d_6; δ, ppm): 2.68 (3H, s, CH_3CO), 3.81 (3H, s, CH_3O), 6.61-6.98 (3H, m, $3CH_{ar}$), 7.11-7.48 (2H, m, $2CH_{ar}$), 7.49-7.86 (2H, m, $2CH_{ar}$), 7.93 (1H, d, *J* = 8.5 Hz, 7-CH_{ar}), 8.95 (1H, brs, CH), 11.73 (1H, brs, NH). ^{13}C NMR (DMSO-d_6; δ, ppm): 26.3, 55.0, 102.2, 108.4, 109.3, 116.2, 122.2, 123.2, 124.6, 130.4, 133.3, 135.6, 140.8, 143.2, 160.4, 168.2, 180.0. MS (EI; rel. int., %): m/z 308 (M^+, 88). Anal. calcd for $C_{18}H_{16}N_2O_3$: C, 70.12; H, 5.23; N, 9.09. Found: C, 70.21; H, 5.34; N, 9.14.

1-Acetyl-2-(((3,4-dimethoxyphenyl)amino)methylene)indolin-3-one **12g**

Yield 0.22 g (71 %), white solid, mp 199-200 °C (methanol:DMF). ^{1}H NMR (DMSO-d_6; δ, ppm): 2.67 (3H, s, CH_3CO), 3.75 and 3.83 (3H, s, $2CH_3O$), 6.55-7.16 (3H, m, $3CH_{ar}$), 7.29 (1H, t, *J* = 7.4 Hz, 5-CH_{ar}), 7.48-8.07 (3H, m, $3CH_{ar}$), 8.91 (1H, brs, CH), 11.85 (1H, brs, NH). ^{13}C NMR (DMSO-d_6; δ, ppm): 26.6, 55.9, 56.2, 102.7, 108.3, 113.7, 116.1, 116.5, 122.3, 123.4, 125.2, 133.2, 133.8, 137.0, 43.0, 146.2, 150.2, 168.4, 179.5. MS (EI; rel. int., %): m/z 338 (M^+, 85). Anal. calcd for $C_{19}H_{18}N_2O_4$: C, 67.45; H, 5.36; N, 8.28. Found: C, 67.56; H, 5.45; N, 8.34.

1-Acetyl-2-(((2,5-dimethoxyphenyl)amino)methylene)indolin-3-one **12h**

Yield 0.16 g (47 %), white solid, mp 176-177 °C (methanol). ^{1}H NMR (DMSO-d_6; δ, ppm): 2.69 (3H, s, CH_3CO), 3.76 and 3.89 (3H and 3H, s and s, $2CH_3O$), 6.62 (1H, dd, *J* = 8.9, 2.7 Hz, 3'-CH_{ar}), 6.90 (1H, d, *J* = 2.7 Hz, 6'-CH_{ar}), 7.01 (1H, d, *J* = 8.9 Hz, 4'-CH_{ar}), 7.31 (1H, t, *J* = 7.4 Hz, 6-CH_{ar}), 7.64 (1H, t, *J* = 7.8 Hz, 5-CH_{ar}), 7.77 (1H, d, *J* = 7.6 Hz, 4-CH_{ar}), 7.94 (1H, d, *J* = 8.5 Hz, 7-CH_{ar}), 8.94 (1H, d, *J* = 11.9 Hz, CH), 11.94 (1H, d, *J* = 12.3 Hz, NH). ^{13}C NMR (DMSO-d_6; δ, ppm): 26.5, 55.4, 56.4, 100.2, 107.7, 112.8, 116.3, 116.8, 122.3, 123.3, 124.8, 129.5, 133.3, 134.2, 142.3, 143.2, 154.0, 168.3, 180.0. MS (EI; rel. int., %): m/z 338 (M^+, 92). Anal. calcd for $C_{19}H_{18}N_2O_4$: C, 67.45; H, 5.36; N, 8.28. Found: C, 67.32; H, 5.29; N, 8.16.

1-Acetyl-2-(((3,4,5-trimethoxyphenyl)amino)methylene)indolin-3-one **12i**

Yield 0.25 g (73 %), white solid, mp 219-220 °C (methanol:DMF). ^{1}H NMR (DMSO-d_6; δ, ppm): 2.67 (3H, s, CH_3CO), 3.66 (3H, s, CH_3O), 3.84 (6H, s, $2CH_3O$), 6.58 (2H, s, 2',6'-CH_{ar}), 7.29 (1H, t, *J* = 7.4 Hz, 5-CH_{ar}), 7.52-7.82 (2H, m, $2CH_{ar}$), 7.92 (1H, d, *J* = 8.5 Hz, 7-CH_{ar}), 8.89 (1H, brs, CH), 11,54 (1H, brs, NH). ^{13}C NMR (DMSO-d_6; δ, ppm): 26.3, 55.9, 59.9, 95.9, 116.1, 122.0, 123.2, 124.7, 130.0, 133.0, 134.5, 135.6, 136.2, 143.0, 153.6, 168.1, 179.6. MS (EI; rel. int., %): m/z 368 (M^+, 92). Anal. calcd for $C_{20}H_{20}N_2O_5$: C, 65.21; H, 5.47; N, 7.60. Found: C, 65.15; H, 5.53; N, 7.56.

1-Acetyl-2-(((4-ethoxyphenyl)amino)methylene)indolin-3-one **12j**

Yield 0.24 g (75 %), white solid, mp 156-157 °C (isopropanol). ^{1}H NMR (DMSO-d_6; δ, ppm): 1.33 (3H, t, *J* = 6.9 Hz, CH_3O), 2.69 (3H, s, CH_3CO), 4.01 (2H, q, CH_3CH_2), 6.96 (2H, d, *J* = 8.7 Hz, 3',5'-CH_{ar}), 7.29 (3H, m, $3CH_{ar}$), 7.49-7.85 (2H, m, $2CH_{ar}$), 7.94 (1H, d, *J* = 8.5 Hz, 7-CH_{ar}), 8.95 (1H, brs, CH), 11.91 (1H, brs, NH). ^{13}C NMR (DMSO-d_6; δ, ppm): 14.7, 26.9, 63.3, 115.6, 115.9, 116.5, 118.0, 122.3, 123.5, 125.1, 132.9, 133.1, 137.0, 142.7, 155.4, 168.5, 179.3. MS (EI; rel. int., %): m/z 322 (M^+, 89). Anal. calcd for $C_{19}H_{18}N_2O_3$: C, 70.79; H, 5.63; N, 8.69. Found: C, 70.86; H, 5.56; N, 8.59.

1-Acetyl-2-(((4-butoxyphenyl)amino)methylene)indolin-3-one **12k**

Yield 0.26 g (74 %), white solid, mp 136-137 °C (isopropanol). ^{1}H NMR (DMSO-d_6; δ, ppm): 0.94 (3H, t, *J* = 7.3 Hz, CH_3), 1.44 (2H, hex, 2H, *J* = 7.1 Hz, $CH_3C\underline{H_2}$), 1.69 (2H, quint, *J* = 6.6 Hz, CH_2), 2.67 (3H, s, CH_3CO), 3.95 (2H, t, *J* = 6.3 Hz, CH_2O), 6.95 (2H, d, *J* = 8.6 Hz, $2CH_{ar}$), 7.11-7.41 (3H, m, $3CH_{ar}$), 7.51-7.83 (2H, m, $2CH_{ar}$), 7.91 (1H, d, *J* = 8.4 Hz, 7-CH_{ar}), 8.92 (1H, brs, CH), 11.90 (1H, s, NH). ^{13}C NMR (DMSO-d_6; δ, ppm): 13.6, 18.7, 26.7, 30.8, 67.7, 115.8, 116.0, 116.4, 118.0, 122.3, 123.4, 125.2, 133.1, 137.0, 142.8, 155.7, 168.4, 179.3. MS (EI; rel. int., %): m/z 350 (M^+, 87). Anal. calcd for $C_{21}H_{22}N_2O_3$: C, 71.98; H, 6.33; N, 7.99. Found: C, 72.05; H, 6.24; N, 8.06.

1-Acetyl-2-(((2-(trifluoromethyl)phenyl)amino)methylene)indolin-3-one **12l**

Yield 0.15 g (43 %), white solid, mp 209-210 °C (methanol). ^{1}H NMR (DMSO-d_6; δ, ppm): 2.71 (3H, s, CH_3CO), 7.16-7.50 (2H, m, $2CH_{ar}$), 7.59-7.89 (5H, m, $5CH_{ar}$), 7.98 (1H, d, *J* = 8.5 Hz, 7-CH_{ar}), 9.03 (1H, d, *J* = 11.2 Hz, CH), 12.24 (1H, d, *J* = 11.3 Hz, NH). ^{13}C NMR (DMSO-d_6; δ, ppm): 26.5, 116.3, 116.8, 117.8, 121.3, 122.6, 123.2, 123.5, 124.2, 126.5, 126.6, 126.7, 134.0, 134.1, 134.7, 137.8, 143.8, 168.3, 181.3. MS (EI; rel. int., %): m/z 346 (M^+, 88). Anal. calcd for $C_{18}H_{13}F_3N_2O_2$: C, 62.43; H, 3.78; N, 8.09. Found: C, 62.51; H, 3.69; N, 7.98.

1-Acetyl-2-(((3-(trifluoromethyl)phenyl)amino)methylene)indolin-3-one **12m**

Yield 0.18 g (52 %), white solid, mp 156-157 °C (methanol). ^{1}H NMR (DMSO-d_6; δ, ppm): 2.69 (3H, s, CH_3CO), 7.07-7.51 (2H, m, $2CH_{ar}$), 7.52-7.86 (5H, m, $5CH_{ar}$), 7.95 (1H, d, *J* = 8.5 Hz, 7-CH_{ar}), 8.97 (1H, brs, CH), 11.75 (1H, brs, NH). ^{13}C NMR (DMSO-d_6; δ, ppm): 26.7, 113.0, 113.1, 116.6, 117.0, 119.6, 119.7, 120.1, 122.6, 123.6, 124.6, 130.8, 134.0, 135.0, 140.7, 143.7, 168.6, 180.8. MS (EI; rel. int., %): m/z 346 (M^+, 94). Anal. calcd for $C_{18}H_{13}F_3N_2O_2$: C, 62.43; H, 3.78; N, 8.09. Found: C, 62.54; H, 3.82; N, 7.94.

1-Acetyl-2-(((4-(trifluoromethyl)phenyl)amino)methylene)indolin-3-one **12n**

Yield 0.14 g (40 %), white solid, mp 195-197 °C (methanol). ^{1}H NMR (DMSO-d_6; δ, ppm): 2.67 (3H, s, CH_3CO), 7.14-8.06 (8H, m, $8CH_{ar}$), 8.96 (1H, d, *J* = 11.2 Hz, CH), 11.73 (d, *J* = 11.6 Hz, NH). ^{13}C NMR (DMSO-d_6; δ, ppm): 26.6, 116.1, 116.3, 117.2, 122.5, 123.5, 124.4, 126.7, 133.9, 134.0, 143.0, 143.6, 168.4, 180.9. MS (EI; rel. int., %): m/z 346 (M^+, 95). Anal. calcd for $C_{18}H_{13}F_3N_2O_2$: C, 62.43; H, 3.78; N, 8.09. Found: C, 62.57; H, 3.83; N, 8.01.

1-Acetyl-2-(((3-(trifluoromethoxy)phenyl)amino)methylene)indolin-3-one **12o**

Yield 0.17 g (47 %), white solid, mp 119-120 °C (hexane:isopropanol). ^{1}H NMR (DMSO-d_6; δ, ppm): 2.68 (3H, s, CH_3CO), 7.04 (1H, d, *J* = 8.2 Hz, 4'-CH_{ar}), 7.30 (3H, m, $3CH_{ar}$), 7.50 (1H, t, *J* = 8.1 Hz, 5-CH_{ar}), 7.58-7.84 (2H, m, $2CH_{ar}$), 7.94 (1H, d, *J* = 8.5 Hz, 7-CH_{ar}), 8.91 (1H, d, *J* = 6.2 Hz, CH), 11.67 (1H, brs, NH). ^{13}C NMR (DMSO-d_6; δ, ppm): 26.8, 109.2, 115.2, 116.6, 117.0, 122.6, 123.6, 124.6, 131.4, 134.0, 135.0, 141.7, 143.7, 149.4, 168.6, 180.8. MS (EI; rel. int., %): m/z 362 (M^+, 86). Anal. calcd for $C_{18}H_{13}F_3N_2O_3$: C, 59.67; H, 3.62; N, 7.73. Found: C, 59.74; H, 3.72; N, 7.65.

1-Acetyl-2-(((4-(trifluoromethoxy)phenyl)amino)methylene)indolin-3-one **12p**

Yield 0.20 g (55 %), white solid, mp 179-181 °C (ethyl acetate). ^{1}H NMR (DMSO-d_6; δ, ppm): 2.69 (3H, s, CH_3CO), 7.13-7.57 (5H, m, $5CH_{ar}$), 7.57-7.86 (2H, m, $2CH_{ar}$), 7.94 (1H, d, *J* = 8.5 Hz, 7-

CH_{ar}), 8.93 (1H, brs, CH), 11.77 (1H, brs, NH). ^{13}C NMR (DMSO-d_6; δ, ppm): 26.4, 116.3, 116.7, 117.4, 117.7, 122.1, 122.3, 122.6, 123.3, 124.6, 133.5, 135.4, 138.9, 143.4, 143.9, 168.3, 180.4. MS (EI; rel. int., %): m/z 362 (M^+, 81). Anal. calcd for $C_{18}H_{13}F_3N_2O_3$: C, 59.67; H, 3.62; N, 7.73. Found: C, 59.59; H, 3.54; N, 7.67.

3-(((1-Acetyl-3-oxoindolin-2-ylidene)methyl)amino)benzoic acid ethyl ester **12q**

Yield 0.22 g (63 %), white solid, mp 159-160 °C (isopropanol). ^{1}H NMR (DMSO-d_6; δ, ppm): 1.36 (3H, t, *J* = 7.1 Hz, $C\underline{H_3}CH_2$), 2.69 (3H, s, CH_3CO), 4.35 (2H, q, *J* = 7.1 Hz, $CH_3C\underline{H_2}$), 7.30 (1H, t, *J* = 7.4 Hz, 5-CH_{ar}), 7.42-7.83 (6H, m, 6CH_{ar}), 7.90 (1H, d, *J* = 8.4 Hz, 7-CH_{ar}), 8.99 (1H, s, CH), 11.78 (1H, brs, NH). ^{13}C NMR (DMSO-d_6; δ, ppm): 13.8, 26.3, 60.6, 116.2, 116.7, 120.1, 120.5, 122.3, 123.2, 123.7, 124.5, 129.9, 131.3, 133.4, 135.0, 140.0, 143.3, 164.9, 168.2, 180.4. MS (EI; rel. int., %): m/z 350 (M^+, 75). Anal. calcd for $C_{20}H_{18}N_2O_4$: C, 68.56; H, 5.18; N, 8.00. Found: C, 68.41; H, 5.22; N, 8.06.

3-(((1-Acetyl-3-oxoindolin-2-ylidene)methyl)amino)benzenesulfonamide **12r**

Yield 0.17 g (48 %), white solid, mp 214-215 °C (acetonitrile:DMF). ^{1}H NMR (DMSO-d_6; δ, ppm): 2.70 (3H, s, CH_3CO), 7.16-8.08 (10H, m, 8CH_{ar} & NH_2), 9.05 (1H, brs, CH), 11.84 (1H, brs, NH). ^{13}C NMR (DMSO-d_6; δ, ppm): 26.9, 112.9, 116.6, 117.1, 119.8, 120.3, 122.7, 123.7 124.6, 126.0, 130.6, 134.0, 135.1, 140.3, 143.5, 145.7, 168.7, 180.8. MS (EI; rel. int., %): m/z 357 (M^+, 74). Anal. calcd for $C_{17}H_{15}N_3O_4S$: C, 57.13; H, 4.23; N, 11.76. Found: C, 57.21; H, 4.15; N, 11.64.

1-Acetyl-2-((pyridin-2-ylamino)methylene)indolin-3-one **12s**

Yield 0.21 g (73 %), white solid, mp 162-164 °C (methanol). ^{1}H NMR (DMSO-d_6; δ, ppm): 2.67 (3H, s, CH_3CO), 6.90-7.49 (3H, m, 3CH_{ar}), 7.51-8.07 (4H, m, 4CH_{ar}), 8.35 (1H, t, *J* = 5.9 Hz, 7-CH_{ar}), 9.47 (1H, d, *J* = 11.4 Hz, CH), 11.76 (1H, d, *J* = 11.5 Hz, NH). ^{13}C NMR (DMSO-d_6; δ, ppm): 27.0, 111.9, 116.5, 117.4, 118.8, 122.7, 123.5, 124.5, 132.9, 134.0, 138.8, 143.8, 148.3, 151.1, 168.4, 181.3. MS (EI; rel. int., %): m/z 279 (M^+, 64). Anal. calcd for $C_{16}H_{13}N_3O_2$: C, 68.81; H, 4.69; N, 15.05. Found: C, 68.89; H, 4.78; N, 15.11.

1-Acetyl-2-((pyridin-4-ylamino)methylene)indolin-3-one **12t**

Yield 0.04 g (30 %), white solid, mp 267-268 °C (decomp.) (methanol). ^{1}H NMR (DMSO-d_6; δ, ppm): 2.69 (3H, s, CH_3CO), 7.19-7.41 (3H, m, 3CH_{ar}), 7.59-7.86 (2H, m, 2CH_{ar}), 7.95 (1H, d, *J* = 8.5 Hz, CH_{ar}), 8.44 (2H, d, *J* = 6.0 Hz, 2CH_{ar}), 8.95 (1H, d, *J* = 11.6 Hz, CH), 12.0 (1H, d, *J* = 12.0 Hz, NH). ^{13}C NMR (DMSO-d_6; δ, ppm): 26.3, 110.4, 116.4, 117.7, 122.5, 123.5, 124.1, 132.7, 134.2, 144.2, 14.2, 150.5, 168.4, 181.6. MS (EI; rel. int., %): m/z 279 (M^+, 59). Anal. calcd for $C_{16}H_{13}N_3O_2$: C, 68.81; H, 4.69; N, 15.05. Found: C, 68.77; H, 4.74; N, 15.08.

1-Acetyl-2-(((3-benzylphenyl)amino)methylene)indolin-3-one **12u**

Yield 0.25 g (68 %), white solid, mp 154-155 °C (isopropanol). ^{1}H NMR (DMSO-d_6; δ, ppm): 2.68 (3H, s, CH_3CO), 3.96 (2H, s, CH_2), 6.97 (1H, d, *J* = 7.5 Hz, CH_{ar}), 7.04-7.49 (9H, m, 9CH_{ar}), 7.65 (1H, t, *J* = 7.4 Hz, 5-CH_{ar}), 7.77 (1H, d, *J* = 7.5 Hz, 4-CH_{ar}), 7.92 (1H, d, *J* = 8.5 Hz, 7-CH_{ar}), 8.99 (1H, brs, CH), 11.81 (1H, brs, NH). ^{13}C NMR (DMSO-d_6; δ, ppm): 26.8, 40.9, 113.9, 116.4, 116.5, 116.7, 122.4, 123.5, 124.3, 124.8, 126.0, 128.4, 128.7, 129.9, 133.5, 136.0, 139.7, 140.8, 143.1,

143.2, 168.5, 180.0. MS (EI; rel. int., %): m/z 368 (M^+, 83). Anal. calcd for $C_{24}H_{20}N_2O_2$: C, 78.24; H, 5.47; N, 7.60. Found: C, 78.15; H, 5.54; N, 7.54.

1-Acetyl-2-(((4-benzylphenyl)amino)methylene)indolin-3-one **12v**

Yield 0.21 g (57 %), white solid, mp 143-145 °C (ethyl acetate). ^{1}H NMR (DMSO-d_6; δ, ppm): 2.67 (3H, s, CH_3CO), 3.91 (2H, s, CH_2), 7.03-7.46 (10H, m, $10CH_{ar}$), 7.49-7.84 (2H, m, $2CH_{ar}$), 7.92 (1H, d, J = 8.5 Hz, 7-CH_{ar}), 8.99 (1H, d, J = 9.6 Hz, CH), 11.85 (1H, d, J = 11.9 Hz, NH). ^{13}C NMR (DMSO-d_6; δ, ppm): 26.8, 40.3, 116.2, 116.5, 122.4, 123.5, 124.9, 125.9, 128.4, 128.6, 130.0, 133.4, 136.2, 137.0, 137.7, 141.2, 143.0, 168.5, 179.8. MS (EI; rel. int., %): m/z 368 (M^+, 89). white solid, Anal. calcd for $C_{24}H_{20}N_2O_2$: C, 78.24; H, 5.47; N, 7.60. Found: C, 78.32; H, 5.36; N, 7.64.

1-Acetyl-2-(((3-phenoxyphenyl)amino)methylene)indolin-3-one **12w**

Yield 0.27 g (68 %), white solid, mp 149-150 °C (isopropanol). ^{1}H NMR (DMSO-d_6; δ, ppm): 2.66 (3H, s, CH_3CO), 6.85-7.20 (5H, m, $5CH_{ar}$), 7.20-7.43 (5H, m, $5CH_{ar}$), 7.62 (1H, t, J = 7.7 Hz, 5-CH_{ar}), 7.73 (1H, d, J = 7.5 Hz, 4-CH_{ar}), 7.87 (1H, d, J = 8.5 Hz, 7-CH_{ar}), 8.94 (1H, brs, CH), 11.86 (1H, brs, NH). ^{13}C NMR (DMSO-d_6; δ, ppm): 26.9, 116.3, 116.5, 118.1, 120.3, 122.4, 12.2, 123.5, 124.9, 130.0, 133.4, 135.6, 136.4, 143.0, 152.7, 157.1, 168.5, 179.8. MS (EI; rel. int., %): m/z 370 (M^+, 74). Anal. calcd for $C_{23}H_{18}N_2O_3$: C, 74.58; H, 4.90; N, 7.56. Found: C, 74.67; H, 4.85; N, 7.44.

1-Acetyl-2-(((4-(phenylamino)phenyl)amino)methylene)indolin-3-one **12x**

Yield 0.27 g (73 %), white solid, mp 184-185 °C (isopropanol:DMF). ^{1}H NMR (DMSO-d_6; δ, ppm): 2.70 (3H, s, CH_3CO), 6.81 (1H, t, J = 7.2 Hz, 5-CH_{ar}), 6.96-7.41 (9H, m, $9CH_{ar}$), 7.65 (1H, t, J = 8.5 Hz, 6-CH_{ar}), 7.78 (1H, d, J = 7.7 Hz, 4-CH_{ar}), 7.94 (1H, d, J = 8.5 Hz, 7-CH_{ar}), 8.21 (1H, brs, NH), 8.99 (1H, s, CH), 12.02 (1H, brs, NH). ^{13}C NMR (DMSO-d_6; δ, ppm): 26.9, 115.8, 116.4, 117.9, 118.2, 119.6, 122.2, 123.5, 125.1, 129.2, 132.2, 133.1, 136.8, 140.1, 142.6, 143.4, 168.6, 179.0. MS (EI; rel. int., %): m/z 369 (M^+, 91). Anal. calcd for $C_{23}H_{19}N_3O_2$: C, 74.78; H, 5.18; N, 11.37. Found: C, 74.69; H, 5.11; N, 11.32.

1-Acetyl-5-methoxy-2-(((4-methoxyphenyl)amino)methylene)indolin-3-one **13a**

Yield 0.12 g (48 %), white solid, mp 161-162 °C (methanol). ^{1}H NMR (DMSO-d_6; δ, ppm): 2.62 (3H, s, CH_3CO), 3.76 (3H, s, CH_3O), 3.82 (3H, s, CH_3O), 6.96 (2H, d, J = 8.8 Hz, 2',6'-CH_{ar}), 7.20 (4H, m, $4CH_{ar}$), 7.79 (d, J = 9.4 Hz, 7-CH_{ar}), 8.89 (1H, brs, CH), 11.55 (1H, brs, NH). ^{13}C NMR (DMSO-d_6; δ, ppm): 26.6, 55.3, 55.6, 103.9, 115.1, 116.4, 117.7, 118.1, 121.4, 126.0, 133.0, 137.2, 155.7, 156.1, 168.0, 179.0. MS (EI; rel. int., %): m/z 338 (M^+, 86). Anal. calcd for $C_{19}H_{18}N_2O_4$: C, 67.45; H, 5.36; N, 8.28. Found: C, 67.52; H, 5.42; N, 8.21.

3-(((1-Acetyl-5-methoxy-3-oxoindolin-2-ylidene)methyl)amino)benzoic acid ethyl ester **13b**

Yield 0.09 g (32 %), white solid, mp 169-170 °C (methanol). ^{1}H NMR (DMSO-d_6; δ, ppm): 1.35 (3H, t, J = 7.1 Hz, $C\underline{H_3}CH_2$), 2.62 (3H, s, CH_3CO), 3.80 (3H, s, CH_3O), 4.33 (2H, q, J = 7.1 Hz, $CH_3C\underline{H_2}$), 7.17 (2H, dd, J = 12.9, 3.9 Hz, $2CH_{ar}$), 7.33-7.95 (5H, m, $5CH_{ar}$), 8.94 (1H, d, J = 10.8 Hz, CH), 11.72 (1H, d, J = 11.8 Hz, NH). ^{13}C NMR (DMSO-d_6; δ, ppm): 14.0, 26.4, 55.7, 60.9, 104.5, 116.5, 117.4, 120.8, 121.9, 123.9, 125.8, 130.1, 131.6, 135.3, 138.1, 140.2, 155.9, 165.2,

167.9, 180.4. MS (EI; rel. int., %): m/z 380 (M^+, 89). Anal. calcd for $C_{21}H_{20}N_2O_5$: C, 66.31; H, 5.30; N, 7.36. Found: C, 66.23; H, 5.36; N, 7.27.

1-Acetyl-5-chloro-2-(((4-methoxyphenyl)amino)methylene)indolin-3-one **14a**

Yield 0.08 g (45 %), white solid, p 167-168 °C (isopropanol). ^{1}H NMR (DMSO-d_6; δ, ppm): 2.67 (3H, s, CH_3CO), 3.77 (3H, s, CH_3O), 6.98 (2H, d, J = 8.9 Hz, 3',5'-CH_{ar}), 7.26 (2H, d, J = 8.7 Hz, 2',6'-CH_{ar}), 7.49-7.82 (2H, m, 4,5-CH_{ar}), 7.96 (1H, d, J = 8.9 Hz, 7-CH_{ar}), 8.89 (1H, brs, CH). ^{13}C NMR (DMSO-d_6; δ, ppm): 26.5, 55.5, 115.7, 116.3, 118.4, 121.3, 126.6, 128.1, 132.4, 132.9, 137.9, 141.2, 156.6, 168.1, 171.5. MS (EI; rel. int., %): m/z 342 (M^+, 69). Anal. calcd for $C_{18}H_{15}ClN_2O_3$: C, 63.07; H, 4.41; N, 8.17. Found: C, 63.11; H, 4.53; N, 8.12.

3-(((1-Acetyl-5-chloro-3-oxoindolin-2-ylidene)methyl)amino)benzoic acid ethyl ester **14b**

Yield 0.1 g (50 %), white solid, mp 175-176 °C (isopropanol). ^{1}H NMR (DMSO-d_6; δ, ppm): 1.37 (3H, t, J = 7.1 Hz, CH_3CH_2), 2.68 (3H, s, CH_3CO), 4.37 (2H, q, J = 7.1 Hz, CH_3CH_2), 7.38-7.83 (6H, m, 6CH_{ar}), 7.96 (1H, d, J = 8.9 Hz, 7-CH_{ar}), 8.97 (1H, brs, CH), 11.80 (1H, brs, NH). ^{13}C NMR (DMSO-d_6; δ, ppm): 13.9, 26.3, 60.7, 116.7, 117.1, 118.2, 120.9, 121.5, 124.2, 126.1, 128.1, 130.0, 131.5, 132.9, 136.0, 139.9, 141.8, 165.0, 168.3, 178.7. MS (EI; rel. int., %): m/z 384 (M^+, 73). Anal. calcd for $C_{20}H_{17}ClN_2O_4$: C, 62.42; H, 4.45; N, 7.28. Found: C, 62.34; H, 4.52; N, 7.15.

General procedure for the synthesis of 1-acetyl-2-((arylamino)methylene)-1,2-dihydro-3*H*-pyrrolo[2,3-*b*]pyridin-3-ones 18a-d

A mixture of 1-acetyl-1,2-dihydro-3*H*-pyrrolo[2,3-*b*]pyridin-3-one **17** (1.0 eqv) and piperidine-carboxaldehyde dimetylacetal (2.5 eqv) in benzene (6 mL) was stirred at room temperature for 3 h. After completion of the reaction (monitored by TLC using benzene:methanol 9:1 as an eluent), the reaction mixture was concentrated *in vacuo*, and the corresponding aniline (1.1 eqv) and AcOH (3.0 mL) in isopropanol (6 mL) was added to the residue. The resulting reaction mixture was stirred at room temperature for 2-24 h. The precipitate was filtered off, washed with isopropanol and diethyl ether, and recrystallized from the corresponding solvent to afford the product as a white solid.

1-Acetyl-2-(((2-methoxyphenyl)amino)methylene)-1,2-dihydro-3*H*-pyrrolo[2,3-*b*]pyridin-3-one **18a**

Yield 0.07 g (44 %), white solid, mp 171-172 °C (methanol). ^{1}H NMR (DMSO-d_6; δ, ppm): 2.88 (3H, s, CH_3CO), 3.77 (3H, s, CH_3O), 7.00 (2H, d, J = 8.4 Hz, 3',5'-CH_{ar}), 7.23-7.45 (3H, m, 3CH_{ar}), 8.21 (1H, d, J = 7.5 Hz, 4-CH_{ar}), 8.66 (1H, s, 6-CH_{ar}), 9.18 (1H, brs, CH), 11.89 (1H, brs, NH). ^{13}C NMR (DMSO-d_6; δ, ppm): 27.0, 55.2, 115.0, 115.5, 116.6, 117.9, 119.2, 131.2, 131.3, 132.1, 137.6, 151.5, 154.1, 156.2, 168.4, 176.4. MS (EI; rel. int., %): m/z 309 (M^+, 82). Anal. calcd for $C_{16}H_{15}N_3O_2$: C, 68.31; H, 5.37; N, 14.94. Found: C, 68.23; H, 5.43; N, 14.83.

3-(((1-Acetyl-3-oxo-1,3-dihydro-2*H*-pyrrolo[2,3-*b*]pyridin-2-ylidene)methyl)amino)benzoic acid ethyl ester **18b**

Yield 0.13 g (33 %), white solid, mp 152-153 °C (isopropanol). ^{1}H NMR (DMSO-d_6; δ, ppm): 1.35 (3H, t, J = 7.1 Hz, CH_3CH_2), 2.83 (3H, s, CH_3CO), 4.33 (2H, q, J = 7.1 Hz, CH_3CH_2), 7.16-7.87 (5H, m, 5CH_{ar}), 8.10 (1H, d, J = 7.6 Hz, 4-CH_{ar}), 8.57 (1H, d, J = 4.7 Hz, 6-CH_{ar}), 9.11 (1H, brs, CH),

11.92 (1H, brs, NH). ^{13}C NMR (DMSO-d_6; δ, ppm): 13.8, 27.0, 60.6, 116.1, 116.3, 116.7, 119.3, 120.6, 124.0, 129.9, 131.3, 131.6, 135.6, 139.7, 152.1, 154.7, 164.8, 168.5, 177.8. MS (EI; rel. int., %): m/z 351 (M^+, 88). Anal. calcd for $C_{19}H_{17}N_3O_4$: C, 64.95; H, 4.88; N, 11.96. Found: C, 64.84; H, 4.76; N, 11.81.

1-Acetyl-2-(((3-fluorophenyl)amino)methylene)-1,2-dihydro-3*H*-pyrrolo[2,3-*b*]pyridin-3-one **18c**

Yield 0.06 g (18 %), mp 154-155 °C (isopropanol). ^{1}H NMR (DMSO-d_6; δ, ppm): 2.81 (3H, s, CH_3CO), 6.88 (1H, td, *J* = 8.6 Hz, 2.2 Hz, 5'-CH_{ar}), 6.07-7.21 (2H, m, 2CH_{ar}), 7.21-7.57 (2H, m, 2CH_{ar}), 8.10 (1H, dd, *J* = 7.7, 1.7 Hz, 4-CH_{ar}), 8.58 (1H, dd, *J* = 4.8, 1.7 Hz, 6-CH_{ar}), 9.06 (1H, d, *J* = 10.3 Hz, CH),11.58 (1H, d, *J* = 11.0 Hz, NH). ^{13}C NMR (DMSO-d_6; δ, ppm): 27.5, 103.4, 103.9, 110.1, 110.5, 112.4, 116.4, 116.9, 119.6, 131.4, 131.6, 131.9, 135.9, 141.3, 141.6, 152.4, 154.9, 160.5, 165.4, 168.7, 178.0. MS (EI; rel. int., %): m/z 297 (M^+, 91). Anal. calcd for $C_{16}H_{12}FN_3O_2$: C, 64.64; H, 4.07; N, 14.13. Found: C, 64.76; H, 4.15; N, 14.04.

1-Acetyl-2-(((3-benzylphenyl)amino)methylene)-1,2-dihydro-3*H*-pyrrolo[2,3-*b*]pyridin-3-one **18d**

Yield 0.17 g (38 %), white solid, mp 128-130 °C (methanol). ^{1}H NMR (DMSO-d_6; δ, ppm): 2.83 (3H, s, CH_3CO), 3.95 (2H, s, CH_2), 7.82-7.48 (10H, m, 10CH_{ar}), 8.12 (1H, dd, *J* = 7.6 Hz, 1.7, 4-CH_{ar}), 8.57 (1H, dd, *J* = 4.8, 1.7 Hz, 6-CH_{ar}), 9.14 (1H, d, *J* = 11.9 Hz, CH), 11.73 (1H, d, *J* = 12.0 Hz, NH). ^{13}C NMR (DMSO-d_6; δ, ppm): 27.5, 40.9, 113.9, 116.0, 116.8, 117.1, 119.5, 124.6, 126.0, 128.4, 128.7, 129.9, 131.8, 136.6, 139.5, 140.8, 143.2, 152.1, 154.5, 168.7, 177.4. MS (EI; rel. int., %): m/z 369 (M^+, 85). Anal. calcd for $C_{23}H_{19}N_3O_2$: C, 74.78; H, 5.18; N, 11.37. Found: C, 74.83; H, 5.26; N, 11.45.

Biology

Screening for Activity against Influenza Virus A Neuraminidase

Cell and Viruses. Influenza virus A/PR/9/34 (A/PR/8/34; Institute for Virology, Philipps University Marburg, Germany) and influenza virus A/Jena/5258/09) (isolated and kindly provided by Andy Krumbholz) were grown and titrated in Madin Darby canine Kidney (MDCK; Friedrich Löffler Institute; Germany) cells and proven to be sensitive to oseltamivir and zanamivir previously. [58-60].

Chemiluminescence (CL)-Based Neuraminidase Inhibition Assay. NA activity was determined in 96-well white U-bottom microplates (Greiner bio-one GmbH, Frickenhausen, Germany) using the commercial CL-based NA-Star assay (NA-Star Influenza Neuraminidase Inhibitor Resistance Detection Kit, Applied Biosystems, Darmstadt, Germany), according to the manufacturer's instructions with slight modifications as published before [60]. At least three individual experiments were performed for the calculation of the 50% inhibitory concentration of NA with the JASPR curve-fitting software [47]. The 50% Inhibitory concentration was defined as the compound concentration required to reduce the NA enzymatic activity by 50%. Oseltamivir carboxylate (OS) was used as a positive control.

Cell-based Neuraminidase Inhibition assay: was performed with influenza virus A/Jena/5258/09 in human erythrocytes (Institute of Transfusion Medicine, University Hospital Jena, Jena, Germany) as published [60]. At least three individual experiments were performed.

Evaluation of Selected Compounds for Cytotoxicity in MDCK Cells and Activity against Influenza Virus A

Cell and Viruses. Influenza virus A/Puerto Rico/8/34 (H1N1) was propagated in the allantoic cavity of 10- to 12-day-old chicken embryos for 48 h at 36 °C before the experiment. The infectious titre of the virus was determined in Madin-Darby Canine Kidney (MDCK) cells (ATCC-CCL-34) grown in 96-well plates in alpha-Eagle's Minimal Essential Medium (MEM) medium with 10% fetal bovine serum.

Cytotoxicity Assay. MTS assay was performed using the CellTiter 96 AQ_{ueous} One Solution Cell Proliferation Assay kit (Promega, Madison, WI, USA) according to the manufacturer's instructions with slight modifications. MDCK cells were seeded into 96-well culture plates (10^4 cells per well) and incubated in a 5% CO_2 atmosphere at 37 °C for 24 h. To assess the cytotoxicity of the compounds, a series of their 1.5-fold dilutions at concentrations of 400 to 10 µg/mL were prepared in 100 µl of culture medium and added to the wells of the plates. The plates were incubated in a 5% CO_2 atmosphere at 37 °C for 48 h, then the medium was removed, and 20 µl of CellTiter 96 AQ_{ueous} One Solution reagent was added into each well of the 96-well plates containing samples in 100 µl of culture medium. After 30 min at 37°C in a 5% CO_2 atmosphere, optical density at 490 nm was recorded using a Benchmark Plus microplate reader (Bio-Rad, Hercules, CA, USA). An online IC_{50} calculator (www.aatbio.com/tools/ic50-calculator, AAT Bioquest, Pleasanton, CA, USA) was used to plot dose-response curves and calculate CC_{50} values. 50%-Cytotoxic concentration CC_{50} was defined as the compound concentration that destroys 50% of the cells in culture. Each concentration was tested three times.

Influenza Hemagglutination Inhibition Assay. The compounds were dissolved in 0.1 mL DMSO to prepare stock solutions, and final solutions (300.0-4.0 µM) were prepared by adding MEM with 1 µg/mL trypsin. Compounds were incubated with MDCK cells at 36 °C for 1 h. The cell culture was then infected with influenza virus A/Puerto Rico/8/34 (H1N1) (MOI 0.01) and incubated in a 5% CO_2 atmosphere at 36 °C for 24 h. Serial 10-fold dilutions were then prepared and used to infect MDCK cells, and the plates were incubated in a 5% CO_2 atmosphere at 36 °C for 48 h. A virus titre in the supernatant was determined by hemagglutination test using chicken erythrocytes. To do this, 100 µl of culture medium was transferred into wells of round-bottom plates for immunoassays and an equal volume of 1% suspension of chicken erythrocytes in saline was added. The level of virus reproduction in the wells of the panel was assessed by the hemagglutination reaction of erythrocytes. The virus titre was defined as the reciprocal of the highest dilution of the virus capable of inducing a positive hemagglutination reaction. Infectious virus titre was expressed as 50% of the experimental infectious dose of virus ID50 in 0.2 mL. The 50% effective concentration (EC_{50}), defined as the compound concentration offering 50% inhibition of viral infectious titre in

cells compared to placebo, was calculated from the corresponding dose-response curves. Each concentration was tested three times.

Efficacy Studies

Compounds. Oseltamivir phosphate (oseltamivir) [ethyl(3R,4R,5S)-4-acetamido-5-amino-3-(1-ethylpropoxy)-1-cyclohexene-1-carboxylate] was dissolved in sterile distilled water. Compounds **3e** and **12o** were dissolved in 10% Tween 80.

Cells and virus. Madin Darby canine kidney (MDCK) cells (American Type Culture Collection, Manassas, VA) were grown in minimal essential medium (MEM) supplemented with 10% fetal bovine serum (FBS), 5 mM L-glutamine, 25 mM HEPES, 100 U/ml penicillin, 100 μg/ml streptomycin sulfate, and 100 μg/ml kanamycin sulfate in a humidified atmosphere of 5% CO2. Influenza A/California/04/2009 (H1N1)pdm09 was provided by the WHO National Influenza Centre of Russia (St. Petersburg, Russia) and adapted to mice.

Assessment in a Mouse Model. 6 to 8 week-old female, specific pathogen-free BALB/C mice (12–14 g) (Stezar, Vladimir Region, Russia) (n = 13 mice/group) were lightly anesthetized and inoculated intranasally (30 μL/mouse) with 10^4 TCID50/ml of mouse-adapted A/California/04/2009 (H1N1)pdm09 virus in PBS. The treatments were administered to the mice for 5 consecutive days, beginning 4 h before and 4 h after viral inoculation, by oral gavage using dose of 50 mg/kg of body weight/day for compounds 6202 and 6021 and dose of 20 mg/kg of body weight/day for oseltamivir, which were given twice daily. The placebo was administered in parallel with the antiviral treatments. Mice were monitored for 16 dpi for morbidity and mortality. Weight was measured daily for 5 consecutive days postinfection and then every other day for the rest of the study period. Animals that lost 30% or more of their initial body weight were euthanized. The weight loss or gain was calculated for each mouse as a percentage of its weight on day 0 before the virus inoculation. The reported values are the average percentage changes in weight

All studies with animals were approved by the Mechnikov Research Institute of Vaccines and Sera Committee on the Ethics of Animal Experiments and were conducted in strict accordance with the applicable laws and guidelines (Study number 63/2024).

Viral Pulmonary Titers. Whole lungs of mice from the compound efficacy experiments (n = 3/group) were harvested under sterile conditions on 4 day after virus inoculation, thoroughly rinsed with sterile PBS, homogenized, and resuspended in 1 mL of cold sterile PBS. Lung homogenates were cleared of cellular debris by centrifugation at 2000g for 10 min. The supernatants were serially diluted and inoculated into 96-well plates with confluent monolayers of MDCK cells to determine the TCID50. Virus titers in mouse lungs were calculated as the mean log10 TCID50/mL.

Computational Studies

Molecular Dynamics Simulations

Classical molecular dynamics simulations were performed for complexes of neuraminidase from strain H1N1 and starting compounds **1a-d**, and leading compounds from series **3**, **7**, **12.** The

source of coordinates of heavy atoms was a crystal structure PDB ID: 3B7E [13]. Hydrogen atoms were added assuming neutral pH for all ionisable groups. CHARMM36 force field parameters were utilized for a protein macromolecule [51,52]. CGenFF was utilized for ligands parameterization [53]. The model system was prepared as follows. For each considered compound, 10 ligand molecules were randomly placed so that the distance between the protein surface and a ligand is larger than 7 Å. Such systems were solvated in a rectangular water box so that the distance to border exceeded 15 Å. Then, systems were neutralized by adding sodium or chloride ions. MD simulations were performed at T = 300 K and p = 1 atm. Several runs were performed with the total length of 400 ns for each compound. MD trajectories were analyzed for the presence of binding sites. After that a novel set of model systems was considered. Each of these systems carried a complex of a protein with a ligand being bound to the protein in one of the binding sites found at the previous step. These MD simulations were performed for 100 ns. We monitored interactions between the enzyme and inhibitor and assigned interactions to the stable binding site if a ligand remained bound for more than 50 ns. RMSD over heavy protein atoms was calculated to be sure that the system is equilibrated and no additional processes occur in the protein-ligand complex. Protein-ligand interactions discussed in the results section were stable for the length of the whole MD run. MD simulations were performed using a NAMD3 program [54].

Machine Learning

Public data from ChEMBL [55] was obtained for compounds screened against influenza H1N1 (CHEMBL613740) and neuraminidase (ChEMBL6135) and used to generate Bayesian machine learning models with Assay Central software and the extended connectivity fingerprint (ECFP6) descriptors as described previously [56]. Various metrics for internal predictive performance were generated after five-fold cross-validation: Recall, Precision, Specificity, F1-Score, Receiver Operating Characteristic (ROC) curve, Cohen's Kappa, and the Matthews Correlation Coefficient. These models were then used to score the compounds generated in this project. Assay Central predictions include both a probability-like score (values > 0.5 considered an active prediction) and an applicability score to assesses the representation of the predicted molecule within the training set. Additional model building with further machine learning algorithms was attempted (see Supplementary Materials).

Physicochemical Properties Calculations

The SwissADME web tool (http://www.swissadme.ch/, SIB Swiss Institute of Bioinformatics, Lausanne, Switzerland) was used to calculate the lipophilicity Log *P* and the polarity (topological polar surface area (TPSA)) for hit compounds. The consensus Log $P_{o/w}$, the arithmetic mean of the values predicted by the five proposed methods, was used [57].

Associated Content

Data Availability

Data supporting the findings of this study are presented in the paper or the Supplementary Materials.

Notes:

SE is owner, TRL is an employee at Collaborations Pharmaceuticals, Inc. Other authors declare no competing financial interest.

Acknowledgements

SE kindly acknowledges Ms. Kimberley Zorn, Mr. Daniel Foil and Dr. Alex Clark for assistance with earlier machine learning model building. Dr. Mindy Davis and Dr. Amanda Ulloa are kindly acknowledged for their support with the NIAID virus *in vitro* testing and screening capabilities. We also thank Dr. Anna Egorova (Federal Research Centre “Fundamentals of Biotechnology” of the Russian Academy of Sciences, Russia) for the fruitful discussion during the drafting of the manuscript.

Funding

This work was supported by the Russian Science Foundation under grant 24-15-00066 (AT, NM, VM) by a grant from National Institutes of General Medical Sciences grant: R44GM122196 (SE), and a grant from National Institute of Environmental Health Sciences grant: R44ES031038 (SE). The National Institute of Allergy and Infectious Diseases (NIAID) program for non-clinical and pre-clinical services is kindly acknowledged (SE).

Abbreviations Used

CL, chemiluminescence; *m*-CPBA, *m*-chloroperoxybenzoic acid; DMAP, 4-dimethylaminopyridine; DME; 1,2-dimethoxyethane; DMF, *N*,*N*-dimethylformamide; HA, hemagglutination; IVA, influenza virus A; MDCK cells, Madin-Darby canine kidney cells; NA, neuraminidase; SA, sialic acid; SASA, solvent-accessible surface area.

References

1. Javanian, M.; Barary, M.; Ghebrehewet, S.; Koppolu, V.; Vasigala, V.; Ebrahimpour, S. A brief review of influenza virus infection. *J. Med. Virol*. **2021**, *93*, 4638-4646. DOI: 10.1002/jmv.26990.
2. Layne, S.P.; Monto, A.S.; Taubenberger, J.K. Pandemic influenza: an inconvenient mutation. *Science*, **2009**, *323*, 1560-15611. DOI: 10.1126/science.323.5921.1560.

3. Dou, D.; Revol, R.; Östbye, H.; Wang, H.; Daniels, R. Influenza A virus cell entry, replication, virion assembly and movement. *Front. Immunol*. **2018**, *9*, 1581. DOI: 10.3389/fimmu.2018.01581.
4. Mahal, A.; Duan, M.; Zinad, D.S.; Mohapatra, R.K.; Obaidullah, A.J.; Wei, X; Pradhan, M.K.; Das, D.; Kandi, V.; Zinad, H.S.; Zhu, Q. Recent progress in chemical approaches for the development of novel neuraminidase inhibitors. *RSC Adv*. **2021**, *11*, 1804-1840. DOI: 10.1039/d0ra07283d.
5. Bassetti, M.; Castaldo, N.; Carnelutti, A. Neuraminidase inhibitors as a strategy for influenza treatment: pros, cons and future perspectives. *Expert Opin. Pharmacother*. **2019**, *20*, 1711-1718. DOI: 10.1080/14656566.2019.1626824.
6. Centers for Disease Control and Prevention. Influenza Antiviral Medications: Summary for Clinicians. https://www.cdc.gov/flu/professionals/antivirals/summary-clinicians.htm (accessed Dec 12, 2022).
7. Thorlund, K.; Awad, T.; Boivin, G.; Thabane, L. Systematic review of influenza resistance to the neuraminidase inhibitors. *BMC Infect. Dis*. **2011**, *11*, 134. DOI: 10.1186/1471-2334-11-134.
8. Lee, N.; Hurt, A.C. Neuraminidase inhibitor resistance in influenza: a clinical perspective. *Curr. Opin. Infect. Dis*. **2018**, *31*, 520-526. DOI: 10.1097/QCO.0000000000000498.
9. Whitley, R.J.; Monto, A.S. Resistance of influenza virus to antiviral medications. *Clin. Infect. Dis*. **2020**, *71*, 1092-1094. DOI: 10.1093/cid/ciz911.
10. Russell, R.J.; Haire, L.F.; Stevens, D.J.; Collins, P.J.; Lin, Y.P.; Blackburn, G.M.; Hay, A.J.; Gamblin, S.J.; Skehel, J.J. The structure of H5N1 avian influenza neuraminidase suggests new opportunities for drug design. *Nature*. **2006**, *443*, 45-49. DOI: 10.1038/nature05114.
11. Amaro, R.E.; Swift, R.V.; Votapka, L.; Li, W.W.; Walker, R.C.; Bush, R.M. Mechanism of 150-cavity formation in influenza neuraminidase. *Nat. Commun*. **2011**, *2*, 388. DOI: 10.1038/ncomms1390.
12. World Health Organization. Influenza (Avian and other zoonotic). https://www.who.int/news-room/fact-sheets/detail/influenza-(avian-and-other-zoonotic) (accessed Dec 12, 2022).
13. Xu, X.; Zhu, X.; Dwek, R.A.; Stevens, J.; Wilson, I.A. Structural characterization of the 1918 influenza virus H1N1 neuraminidase. *J. Virol*. **2008**, *82*, 10493-10501. DOI: 10.1128/JVI.00959-08.
14. Amaro, R.E.; Minh, D.D.; Cheng, L.S.; Lindstrom, W.M. Jr.; Olson, A.J.; Lin, J.H.; Li, W.W.; McCammon, J.A. Remarkable loop flexibility in avian influenza N1 and its implications for antiviral drug design. *J. Am. Chem. Soc*. **2007**, *129*, 7764-7765. DOI: 10.1021/ja0723535.
15. Amaro, R.E.; Cheng, X.; Ivanov, I.; Xu, D.; McCammon, J.A. Characterizing loop dynamics and ligand recognition in human- and avian-type influenza neuraminidases via generalized born molecular dynamics and end-point free energy calculations. *J. Am. Chem. Soc*. **2009**, *131*, 4702-4709. DOI: 10.1021/ja8085643.

16. Air, G.M. Influenza neuraminidase. *Influenza Other Respir. Viruses*. **2012**, *6*, 245-256. DOI: 10.1111/j.1750-2659.2011.00304.x.
17. McAuley, J.L.; Gilbertson, B.P.; Trifkovic, S.; Brown, L.E.; McKimm-Breschkin, J.L. Influenza virus neuraminidase structure and functions. *Front Microbiol*. **2019**, *10*, 39. DOI: 10.3389/fmicb.2019.00039.
18. von Itzstein, M. The war against influenza: discovery and development of sialidase inhibitors. *Nat. Rev. Drug. Discov*. **2007**, *6*, 967-974. DOI: 10.1038/nrd2400.
19. De Clercq, E. Antiviral agents active against influenza A viruses. *Nat. Rev. Drug. Discov*. **2006**, *5*, 1015-1025. DOI: 10.1038/nrd2175.
20. Li, Q.; Qi, J.; Zhang, W.; Vavricka, C.J.; Shi, Y.; Wei, J.; Feng, E.; Shen, J.; Chen, J.; Liu, D.; He, J.; Yan, J.; Liu, H.; Jiang, H.; Teng, M.; Li, X.; Gao, G.F. The 2009 pandemic H1N1 neuraminidase N1 lacks the 150-cavity in its active site. *Nat. Struct. Mol. Biol*. **2010**, *17*, 1266-1268. DOI: 10.1038/nsmb.1909.
21. Landon, M.R.; Amaro, R.E.; Baron, R.; Ngan, C.H.; Ozonoff, D.; McCammon, J.A.; Vajda, S. Novel druggable hot spots in avian influenza neuraminidase H5N1 revealed by computational solvent mapping of a reduced and representative receptor ensemble. *Chem. Biol. Drug Des*. **2008**, *71*, 106-116. DOI: 10.1111/j.1747-0285.2007.00614.x.
22. Cheng, L.S.; Amaro, R.E.; Xu, D.; Li, W.W.; Arzberger, P.W.; McCammon, J.A. Ensemble-based virtual screening reveals potential novel antiviral compounds for avian influenza neuraminidase. *J. Med. Chem*. **2008**, *51*, 3878-3894. DOI: 10.1021/jm8001197.
23. Le, L.; Lee, E.H.; Hardy, D.J.; Truong, T.N.; Schulten, K. Molecular dynamics simulations suggest that electrostatic funnel directs binding of Tamiflu to influenza N1 neuraminidases. *PLoS Comput. Biol*. **2010**, *6*, e1000939. DOI: 10.1371/journal.pcbi.1000939.
24. Tran, D.T. T.; Le L.T.; Truong T.N. Discover binding pathways using the sliding binding-box docking approach: application to binding pathways of oseltamivir to avian influenza H5N1 neuraminidase. *J. Comput. Aided Mol. Des*. **2013**, *27*, 689-695. DOI: 10.1007/s10822-013-9675-1.
25. Vavricka, C.J.; Li, Q.; Wu, Y.; Qi, J.; Wang, M.; Liu, Y.; Gao, F.; Liu, J.; Feng, E.; He, J.; Wang, J.; Liu, H.; Jiang, H.; Gao, G.F. Structural and functional analysis of laninamivir and its octanoate prodrug reveals group specific mechanisms for influenza NA inhibition. *PLoS Pathog*. **2011**, *7*, e1002249. DOI: 10.1371/journal.ppat.1002249.
26. Humphrey, W.; Dalke, A.; Schulten, K. VMD: visual molecular dynamics. *J. Mol. Graph*. **1996**, *14(1)*, 33-8, 27-8. DOI: 10.1016/0263-7855(96)00018-5.
27. Ju, H.; Zhang, J.; Sun, Z. S.; Huang, Z.; Qi, W. B.; Huang, B.; Zhan, P.; Liu, X. Y. Discovery of C-1 modified oseltamivir derivatives as potent influenza neuraminidase inhibitors. *Eur. J. Med. Chem*. **2018**, *146*, 220-231. DOI: 10.1016/j.ejmech.2018.01.050
28. Wang, B.; Wang, K.; Meng, P.; Hu, Y.; Yang, F.; Liu, K.; Lei, Z.; Chen, B.; Tian, Y. Design, synthesis, and evaluation of carboxyl-modified oseltamivir derivatives with improved

lipophilicity as neuraminidase inhibitors. *Bioorg. Med. Chem. Lett*. **2018**, *28*, 3477-3482. DOI: 10.1016/j.bmcl.2018.09.014.

29. Ju, H.; Xiu, S.; Ding, X.; Shang, M.; Jia, R.; Huang, B.; Zhan, P.; Liu, X. Discovery of novel 1,2,3-triazole oseltamivir derivatives as potent influenza neuraminidase inhibitors targeting the 430-cavity. *Eur. J. Med. Chem*. **2020**, *187*, 111940. DOI: 10.1016/j.ejmech.2019.111940.
30. Li, M.; Cheng, L.P.; Pang, W.; Zhong, Z.J.; Guo, L.L. Design, synthesis, and biological evaluation of novel acylhydrazone derivatives as potent neuraminidase inhibitors. *ACS Med. Chem. Lett*. **2020**, *11*, 1745-1750. DOI: 10.1021/acsmedchemlett.0c00313.
31. Ai, W.; Zhang, J.; Zalloum, W.A.; Jia, R.; Cherukupalli, S.; Ding, X.; Sun, Z.; Sun, L.; Jiang, X.; Ma, X.; Li, Z.; Wang, D.; Huang, B.; Zhan, P.; Liu, X. Discovery of novel "Dual-site" binding oseltamivir derivatives as potent influenza virus neuraminidase inhibitors. *Eur. J. Med. Chem*. **2020**, *191*, 112147. DOI: 10.1016/j.ejmech.2020.112147.
32. Malbari, K.; Saha, P.; Chawla-Sarkar, M.; Dutta, S.; Rai, S.; Joshi, M.; Kanyalkar, M. In quest of small-molecules as potent non-competitive inhibitors against influenza. *Bioorg. Chem*. **2021**, *114*, 105139. DOI: 10.1016/j.bioorg.2021.105139.
33. Zima, V.; Albiñana, C.B.; Rojíková, K.; Pokorná, J.; Pachl, P.; Řezáčová, P.; Hudlicky, J.; Navrátil, V.; Majer, P.; Konvalinka, J.; Kožíšek, M.; Machara, A. Investigation of flexibility of neuraminidase 150-loop using tamiflu derivatives in influenza A viruses H1N1 and H5N1. *Bioorg. Med. Chem*. **2019**, *27(13)*, 2935-2947. DOI: 10.1016/j.bmc.2019.05.024. DOI: 10.1016/0263-7855(96)00018-5
34. Ryabova, S.Y.; Trofimkin, Y.I.; Alekseeva, L.M.; Bogdanova, G.A., Sheinker, Yu.N., Granik, V.G. Acetals of lactams and acid amides. 61. Synthesis and transamination of indoxyls and pyrrol-2-in-4-ones. *Chem. Heterocycl. Compd*. **1990**, *26*, 1238-1244 DOI: 10.1007/BF00476977.
35. Isakovich, I.P.; Azimov, V.A.; Ryabova, S.Y.; Alekseeva, L.M.; Parshin, V.P.; Syubaev, R.D.; Parimbetova, R.B.; Asnina, V.V.; Salimova, I.S.; Granik, V.G. Synthesis and pharmacological activity of derivatives of 3-aminomethylene-1-(2′,6′-dichlorophenyl)oxindole and 2-aminomethyleneindoxyl. *Pharm. Chem. J*. **1995**, *29*, 100-105. DOI: 10.1007/BF02226519.
36. Sitkina, L.M.; Dubonosov, A.D.; Lyubarska, A.É.; Bren', V.A.; Minkin, V.I. Benzenoid-quinone tautomerism in azomethines and their structural analogs. 34. 3-hydroxy-1-methylindole-2-carbaldehyde imines. *Chem. Heterocycl. Compd*. **1985**, *21*, 763-766. DOI: 10.1007/BF00519142.
37. Kalgutkar, A.S.; Jones, R.; Sawant, A. Chapter 5. Sulfonamide as an essential functional group in drug design. In Metabolism, Pharmacokinetics and Toxicity of Functional Groups: Impact of Chemical Building Blocks on ADMET; Smith, D.A., Ed.; The Royal Society of Real Chemistry, 2010; pp 210-275. DOI: 10.1039/9781849731102-00210.

38. Clark, M.P.; Ledeboer, M.W.; Davies, I.; Byrn, R.A.; Jones, S.M.; Perola, E.; Tsai, A.; Jacobs, M.; Nti-Addae, K.; Bandarage, U.K.; Boyd, M.J.; Bethiel, R.S.; Court, J.J.; Deng, H.; Duffy, J.P.; Dorsch, W.A.; Farmer, L.J.; Gao, H.; Gu, W.; Jackson, K.; Jacobs, D.H.; Kennedy, J.M.; Ledford, B.; Liang, J.; Maltais, F.; Murcko, M.; Wang, T.; Wannamaker, M.W.; Bennett, H.B.; Leeman, J.R.; McNeil, C.; Taylor, W.P.; Memmott, C.; Jiang, M.; Rijnbrand, R.; Bral, C.; Germann, U.; Nezami, A.; Zhang, Y.; Salituro, F.G.; Bennani, Y.L.; Charifson, P.S. Discovery of a novel, first-in-class, orally bioavailable azaindole inhibitor (VX-787) of influenza PB2. *J. Med. Chem*. **2014**, *57*, 6668-6678. DOI: 10.1021/jm5007275.
39. PharmaTimes Online. Janssen's lead coronavirus vaccine shows preclinical promise. https://www.pharmatimes.com/news/janssens_lead_coronavirus_vaccine_shows_preclinical_promise_1348249 (accessed Dec 14, 2022).
40. Richter, M.; Schumann, L.; Walther, E.; Hoffmann, A.; Braun, H.; Grienke, U.; Rollinger, J.M.; von Grafenstein, S.; Liedl, K.R.; Kirchmair, J.; Wutzler, P.; Sauerbrei; A.; Schmidtke, M. Complementary assays helping to overcome challenges for identifying neuraminidase inhibitors. *Future Virol*. **2015**, *10*, 77-88. DOI: 10.2217/fvl.14.97.
41. Nuthakki, V.K.; Mudududdla, R.; Sharma, A.; Kumar, A.; Bharate, S.B. Synthesis and biological evaluation of indoloquinoline alkaloid cryptolepine and its bromo-derivative as dual cholinesterase inhibitors. *Bioorg Chem*. **2019**, *90*, 103062. DOI: 10.1016/j.bioorg.2019.103062.
42. Tighineanu, E.; Chiraleu, F.; Råileanu, D. Double cyclisation of phenylglycine-o-carboxylic acids – I: New stable mesoionic oxazolone. *Tetrahedron*. **1980**, *36*, 1385-1397. DOI: 10.1016/0040-4020(80)85053-8.
43. Sugasawa, T.; Adachi, M.; Sasakura, K.; Kitagawa, A. Aminohaloborane in organic synthesis. 2. Simple synthesis of indoles and 1-acyl-3-indolinones using specific ortho .alpha.-chloroacetylation of anilines. *J. Org. Chem*. **1979**, *44*, 578-586. DOI: 10.1021/jo01318a021.
44. Robinson, M.M.; Robison, B.L. 7-Azaindole. I. Synthesis and Conversion to 7-Azatryptophan and Other Derivatives. *J. Am. Chem. Soc*. **1955**, *77*, 457-460. DOI: 10.1021/ja01607a071.
45. Cheng, X.; Merz, K.H.; Vatter, S.; Christ, J.; Wölfl, S.; Eisenbrand, G. 7,7′-Diazaindirubin – a small molecule inhibitor of casein kinase 2 *in vitro* and in cells. *Bioorg. Med. Chem*. **2014**, *22*, 247-255. DOI: 10.1016/j.bmc.2013.11.031.
46. Desarbre, E.; Mérour, J.Y. Synthesis and reactivity of 1-substituted-3*H*-pyrrolo[2,3-*b*]pyridin-3-one. *Tetrahedron Lett*. **1994**, *35*, 1995-1998. DOI: 10.1016/S0040-4039(00)73031-0.
47. Okomo-Adhiambo, M.; Sleeman, K.; Ballenger K; Nguyen, HT; Mishin, VP; Sheu, TG; Smagala, J; Li, Y; Klimov, AI; Gubareva LV. Neuraminidase inhibitor susceptibility testing in human influenza viruses: a laboratory surveillance perspective. *Viruses*. **2010**, *2(10)*, 2269-2289. DOI: 10.3390/v2102269.

48. Le Guilloux, V.; Schmidtke, P.; Tuffery, P. Fpocket: an open source platform for ligand pocket detection. *BMC Bioinformatics*. **2009**, *10*, 168. DOI: 10.1186/1471-2105-10-168.
49. Case, D.A.; Darden, T.A.; Cheatham, T.E.; Simmerling, C.L.; Wang, J.; Duke, R.E.; Luo, R.; Crowley, M.; Walker, R.C.; Zhang, W.; Merz, K.M.; Wang, B.; Hayik, S.; Roitberg, A.; Seabra, G.; Kolossvary, I.; Wong, K.F.; Paesani, F.; Vanicek, J.; Wu, X.; Brozell, S.R.; Steinbrecher, T.; Gohlke, H.; Yang, L.; Tan, C.; Morgan, J.; Hornak, V.; Cui, G.; Mathews, D.H.; Seetin, M.G.; Sagui, C.; Babin, V.; Luchko, T.; Gusarov, S.; Kovalenko, A.; Kollman, P.A. AMBER 10. **2008**. University of California, San Francisco.
50. Stroganov, O.V.; Novikov, F.N.; Stroylov, V.S.; Kulkov, V.; Chilov, G.G. Lead finder: an approach to improve accuracy of protein-ligand docking, binding energy estimation, and virtual screening. *J. Chem. Inf. Model*. **2008**, *48*, 2371-2385. DOI: 10.1021/ci800166p.
51. Denning, E.J.; Priyakumar, U.D.; Nilsson, L.; Mackerell, A.D. Jr. Impact of 2'-hydroxyl sampling on the conformational properties of RNA: update of the CHARMM all-atom additive force field for RNA. *J Comput Chem*. **2011**, *32(9)*, 1929-43. DOI: 10.1002/jcc.21777.
52. Best, R.B.; Zhu, X.; Shim, J.; Lopes, P.E.; Mittal, J.; Feig, M.; Mackerell, A.D. Jr. Optimization of the additive CHARMM all-atom protein force field targeting improved sampling of the backbone φ, ψ and side-chain χ(1) and χ(2) dihedral angles. *J Chem Theory Comput*. **2012**, *8(9)*, 3257-3273. DOI: 10.1021/ct300400x.
53. Vanommeslaeghe, K.; Hatcher, E.; Acharya, C.; Kundu, S.; Zhong, S.; Shim, J.; Darian, E.; Guvench, O.; Lopes, P.; Vorobyov, I.; Mackerell, A.D. Jr. CHARMM general force field: A force field for drug-like molecules compatible with the CHARMM all-atom additive biological force fields. *J Comput Chem*. **2010**, *31(4)*, 671-90. DOI: 10.1002/jcc.21367.
54. Phillips, J.C.; Hardy, D.J.; Maia, J.D.C.; Stone, J.E.; Ribeiro, J.V.; Bernardi, R.C.; Buch, R.; Fiorin, G.; Hénin, J.; Jiang, W.; McGreevy, R.; Melo, M.C.R.; Radak, B.K.; Skeel, R.D.; Singharoy, A.; Wang, Y.; Roux, B.; Aksimentiev, A.; Luthey-Schulten, Z.; Kalé, L.V.; Schulten, K.; Chipot, C.; Tajkhorshid, E. Scalable molecular dynamics on CPU and GPU architectures with NAMD. *J Chem Phys*. **2020**, *153(4)*, 044130. DOI: 10.1063/5.0014475.
55. Gaulton, A.; Hersey, A.; Nowotka, M.; Bento, A. P.; Chambers, J.; Mendez, D.; Mutowo, P.; Atkinson, F.; Bellis, L.J.; Cibrian-Uhalte, E.; Davies, M.; Dedman, N.; Karlsson, A.; Magarinos, M.P.; Overington, J.P.; Papadatos, G.; Smit, I.; Leach, A.R. The ChEMBL database in 2017. *Nucleic Acids Res*. **2017**, *45*, D945-D954. DOI: 10.1093/nar/gkw1074.
56. Lane, T.R.; Foil, D.H.; Minerali, E.; Urbina, F.; Zorn, K.M.; Ekins, S. Bioactivity Comparison across Multiple Machine Learning Algorithms Using over 5000 Datasets for Drug Discovery. *Mol. Pharm*. **2021**, *18*, 403-415. DOI: 10.1021/acs.molpharmaceut.0c01013.
57. Daina, A.; Michielin, O.; Zoete, V. SwissADME: a free web tool to evaluate pharmacokinetics, drug-likeness and medicinal chemistry friendliness of small molecules. *Sci. Rep*. **2017**, *7*, 42717. DOI: 10.1038/srep42717.

58. Bauer, K.; Richter, M.; Wutzler, P.; Schmidtke, M. Different neuraminidase inhibitor susceptibilities of human H1N1, H1N2, and H3N2 influenza A viruses isolated in Germany from 2001 to 2005/2006. Antiviral Res. **2009**, *82*, 34-41. DOI: 10.1016/j.antiviral.2009.01.006.
59. Kirchmair, J.; Rollinger, J.M.; Liedl, K.R.; Seide,l N.; Krumbholz, A.; Schmidtke, M. Novel neuraminidase inhibitors: identification, biological evaluation and investigations of the binding mode. Future Med Chem. **2011**, *3*, 437-450. DOI: 10.4155/fmc.10.292.
60. Richter, M.; Schumann, L.; Walther, E.; Hoffmann, A.; Braun, H.; Grienke, U.; Schmidtke, M. Complementary Assays Helping to Overcome Challenges for Identifying Neuraminidase Inhibitors. Future Virology, **2015**, *10*, 77–88. DOI: 10.2217/fvl.14.97.

Influenza virus neuraminidase inhibition

in vitro $IC_{50} \leq 0.2$ μM